EXPLORING DIFFERENT NEUTRALINO DARK MATTER ANNIHILATION CHANNELS IN RADIO FREQUENCY EMISSION IN SIMULATED COMA LIKE GALAXY CLUSTER

By

Jemal Regasa Mashura

A THESIS SUBMITTED TO

GRADUATE PROGRAMS OF
ADDIS ABABA UNIVERSITY

IN PARTIAL FULFILLMENT FOR THE REQUIREMENTS
OF THE DEGREE

MASTER OF SCIENCE IN PHYSICS

(ASTRONOMY/ASTROPHYSICS)

ADDIS ABABA, ETHIOPIA

FEBRUARY 2020

ADDIS ABABA UNIVERSITY

GRADUATE PROGRAMS

EXPLORING DIFFERENT NEUTRALINO DARK MATTER ANNIHILATION CHANNELS IN RADIO FREQUENCY EMISSION IN SIMULATED COMA LIKE GALAXY CLUSTER

By

Jemal Regasa Mashura

Approved by the Examining Board:

Dr. Remudin Reshid _____ Signature
Advisor

_____ Signature
Examiner

_____ Signature
Examiner

Date: February 2020

ADDIS ABABA UNIVERSITY

Date: **February 2020**

Author: **Jemal Regasa Mashura**

Title: **Exploring different neutralino dark matter annihilation channels in radio frequency emission in simulated coma like galaxy cluster**

Department: **Deparment of Physics**

Degree: **M.Sc.** Convocation: **August** Year: **2020**

Signature of Author

This Work is Dedicated

to

Table of Contents

Table of Contents v

List of Table viii

List of Figures ix

Acknowledgements xii

Abbreviations xiii

Physical Constants xv

Symbols xvi

Abstract xvii

1 Introduction 1

1.1 Evidence for Dark Matter 7
1.2 Gravtional lensing 7
1.3 The Cosmic Microwave Background Radiation 9
1.4 Rotation curve of a galaxy 10
1.5 Dark matter candidates 12
1.6 Baryonic dark matter 13
1.7 Non-baryonic dark matter 14
1.8 Weakly interacting massive particles (WIMPS) 15
1.9 Massive Astrophysical Compact Halo Objects (MACHOs) 17
1.10 The annular modulation signal 17
1.11 Standard model particles (SMP) 18
1.12 Supper symmetry particles 19
1.13 DM Detection Searches 20
1.14 Direct detection of DM 20
1.15 Indirect detection of DM 20

1.16 Production in laboratory(Detection from particle colliders) 21
1.17 Short Summary of the chapter 21

2 Diffused radio Emission from DM Annihilation Processes in Galaxy Clusters 23

2.1 Introduction 23
2.2 Radio emissions in galaxy clusters 24
2.2.1 Primary electrons 27
2.3 Models for the origin and evolution of particles giving rise to diffuse sources 28
2.4 Non-thermal emission from galaxy clusters 28
2.4.1 Re-accelerated Electrons 29
2.4.2 The secondary electron model 29
2.4.3 Dark matter annihilation/decay processes 30
2.5 The Dark Matter model 31
2.6 Short and brief summary of the chapter 32

3 Data presentation and analysis 33

3.1 Introduction 33
3.2 Data presentation 34
3.3 Dark matter annihilation model 34
3.3.1 DM distribution 35
3.3.2 Magnetic Field and Thermal Plasma Models 35
3.3.3 Electron Source Functions From Neutralino Annihilations . . 36
3.3.4 The equilibrum spectra of emitting particles 37
3.3.5 Synchrotron Emission 38
3.4 Data analysis 39

4 Results and Discussion 41

4.1 Introduction 41
4.2 The distribution of DM within (SGC280) 42
4.3 Radio flux and emission maps 43
4.3.1 Radio flux and emission maps for M_x = 9 GeV 44
4.3.2 Radio flux and emission maps for M_x = 60 GeV 45
4.3.3 Radio flux and emission maps for M_x = 500 GeV 46
4.4 Integrated radio spectrum from diffrent DM annihilation channels . 52

5 Discussion and conclusions 55

Bibliography **57**

List of Tables

List of Figures

1.1 Matter and energy distribution in the universe today 4

1.2 Gravitational lensing concept 8

1.3 NGC 3198 galactic rotation profile (credit: T. S. van Albada). 11

1.4 The three DM detecation methods 20

2.1 Image of radio halos (left) and radio relics (right) showing the extended diffuse radio emission at the cluster center and periphery, respectively 25

2.2 Integrated radio continuum spectrum of the diffuse radio halo source Coma C. The filled dots represent new observations made by (Thierbach et al., 2003) 26

2.3 Graphical representation of multi-wavelength emission from neutralino annihilation process 31

3.1 Magnetic field profiles of the two magnetic field models: Model A and Model B are shown in red dotted line and green solid line, respectively 36

4.1 Density square map of Galaxy Cluster SGC280 obtained by using SPH kernel. 43

4.2 Radio emission maps from light DM mass 9 GeV annihilation into $b\bar{b}$ (left panel) and $\tau^+\tau^-$ (right panel) at 1400 MHz 44

4.3 Radio emission maps from light DM of mass 9 GeV annihilation into $b\bar{b}$ (left panel) and $\tau^+\tau^-$ (right panel) at 4850 MHz 45

4.4 Radio emission maps from an intermidate neutralino mass 60 GeV annihilation into $b\bar{b}$ (left panel) and $\tau^+\tau^-$ (right panel) at 1400 MHz . 46

4.5 Radio emission maps for an intermediate neutralino mass used M_x=60 GeV annihilated in to $b\bar{b}$ (left panel) and $\tau^+\tau^-$ (right panel) at a frequency of 4850 MHz 46

4.6 Radio emission maps for heavy neutralino mass used M_x=500 GeV annihilated in to $b\bar{b}$ (left panel) and $\tau^+\tau^-$ (right panel) at 1400 MHz . 47

4.7 Radio emission maps for heavy neutralino mass used M_x=500 GeV annihilated in to $b\bar{b}$(left panel) and $\tau^+\tau^-$(right panel) at 4850 MHz . 47

4.8 Radio emission maps for neutralino mass used M_x=500 GeV annihilation in to $b\bar{b}$(left panel) and W^-W^+(right panel) at afrequency of 4850 MHz 48

4.9 Radio emission maps for neutralino mass used M_x=500 Gev annihilation in to $\tau^+\tau^-$(left panel) and W^-W^+(right panel) at afrequency of 1400 MHz 48

4.10 The radial distribution of the flux contribution from each boxes for DM mass 9 Gev and annihilation channels $b\bar{b}$ and $\tau^-\tau^+$ represented in black and red colors, at a frequency 1400 MHz (left panel) and a frequency 4850 MHz (right panel) respectively. 49

4.11 The radial distribution of the flux contribution from each boxes for DM mass 60 Gev and annihilation channels $b\bar{b}$ and $\tau^-\tau^+$ represented in black and red colors, at a frequency 1400 MHz (left panel) and a frequency 4850 MHz (right panel) respectively 49

4.12 The radial distribution of the flux contribution from each boxes for DM mass 500 Gev and annihilation channels $b\bar{b}$ and $\tau^-\tau^+$ represented in black and red colors, at a frequency 1400 MHz (left panel) and a frequency 4850 MHz (right panel) respectively 50

4.13 The radial distribution of the flux contribution from each boxes for DM mass 500 GeV, $b\bar{b}$, $\tau^+\tau^-$, $\tau^+\tau^-$ andW^-W^+ (left) and (right) at 1400 MHz respectively. 50

4.14 Flux density from synchrotron emission of $b\bar{b}$ 9 GeV and $\tau^-\tau^+$ 9 GeV in blue and red curves respectively in comparision to the observetional data of radio emission of coma cluster from [54] indicated in green dots 53

4.15 Flux density from synchrotron emission of $b\bar{b}$ 60 GeV and $\tau^{-}\tau^{+}$ 60 GeV in turqouise and violet curves respectively in comparision to the observetional data of radio emission of coma cluster from [54] indicated in green dots 54

4.16 Flux density from synchrotron emission of $b\bar{b}$ 500 GeV and $\tau^{-}\tau^{+}$ 500 GeV in violet and cyan curves respectively in comparision to the observetional data of radio emission of coma cluster from [54] indicated in green dots 54

Acknowledgements

I would like to express my scincere gratitude to my advisor Dr.Remudin Reshid for all the resources he made available and his contribution of valuable suggestions as we carry out this thesis work .
I would like to express my grateful acknowledgment to my instructors.
I would like also to express my appreciation to all my classmate for the memoriable events we have spent during our study.
The support I have obtained from Fitsum, Kiflom, Fantanesh and my friendes, Abel Habte and Murad Yimam on the thesies writing techqunics through Texmaker is all unforgetable, so I thank them all.
Last but not the list, I would like to thank my family especially my wife who always motivate and strengthen me to focus on my studies.

Addis Ababa University

Jemal Regasa Mashura
August, 2019

Abbreviations

WIMPs	Weakly Interacting Massive Particles
ICM	Intera Cluster Medium
DM	Dark Matter
SM	Standard Matter
HE	High Energy
LE	Low Energy
ICS	Inverse Compton Scattering
LHC	Large Hadron Collider
NFW	Navarro-Frenk-White
AGN	Active Galactic Nuclino
HDM	Hot Dark Matter
MACHO	Massive Compact Halo Object
CDM	Cold Dark Matter

SPH	Smooth Particle Hydrodynamics
SED	Spectral Energy Distribution
CTA	Cherenkov Telescope Array
MUSIC	MUltiDark SImulation of galaxy Clusters
SGC280	Simulated Galaxy Cluster 280
MSSM	Minimal Super-symmetric Standard Model
LSP	Lightest Supersymmetry Particle
LAT	Large Area Telescope
DSA	Diffusive Shock Acceleration
HXR	Hard X-Ray
EUV	Extreme Ultra Violet
GRBs	Gamma-Ray Bursts
QCD	Quantum Chromo Dynamics
ISM	Inter-Stellar Medium

Physical Constants

Speed of Light	c = $2.99792458\times\ 10^{8}$ ms^{-2}
Mass of an Electron	Me = 9.10938356×10^{-28} g
Mass of Proton	Mp = 1.67262178×10^{-24} g
Mass of the Sun	$M\odot$ = $1.99\ \times\ 10^{33}$ g
Kiloparsec	kpc = 3.08568025×10^{21} cm
Boltzmann constant	k = 1.3806505×10^{-23} JK^{-1}
Thomson cross section	σ_T = 6.652×10^{-25} cm^2

Symbols

$\frac{dF}{dE}$	Differential flux ph. cm^{-2} s^{-1} GeV^{-1}
M_χ	Neutralinos or DM mass GeV
ρ_{DM}	DM density $M_\odot$ kpc^{-3}
ρ_{GAS}	Gas density $M_\odot$ kpc^{-3}
n_{el}	Number density of Electrons cm^{-2}
D_l	Luminosity distance of the Coma cluster 96 Mpc

Abstract

We studied various dark matter(DM) annihilation channels in radio frequency in order to explore the possibility to interpret the still unknown origin of radio emission in coma like simulated galaxy clusters. We consider three different DM models with light (9 GeV), intermediate (60 GeV), and high (500 GeV) neutralino mass with annihilation cross-section times velocity of $1.0 \times 10^{-26}\ cm^3 s^{-1}$. We predict radio emission from non-thermal scenario when DM annihilates into different channels such as $b\bar{b}$, $\tau^-\tau^+$ and W^-W^+. The radio emission produced for the three channels in a simulated galaxy cluster is based on the MUSIC-data set. The raw data contain the particle mass and coordinates, which are used to determine the density ρ_i of the DM particle by using Smoothed Particle Hydrodynamics(SPH) kernel. This allows us to easily compute the square of the DM densities integrated in the line-of-sight, revil the observed radio halo morphology showing radio emission both from the centeral regions of the cluster and substructures lying off-center. The radio emission maps and the square of DM density maps were found to be identical proving the fact that higher emission originate from the densest structures. The integrated radio spectrum declines as frequency increases because of the radiative lifetime of the relativistic electrons. The possibility of interpreting the origin of radio emission in galaxy clusters with DM annihilation scenario requires a low neutralino mass.

CHAPTER 1

Introduction

Many years ago, astronomers were calculating the mass of galaxies. They had an idea of how many stars there were, and how much mass those stars represented. Since they knew the approximate mass, they could calculate how fast a galaxy should spin how fast the stars in the arms should be moving. They performed their calculations, then tried to back up the calculations with observations. What they found astonished them in fact, they didn't believe the results. Stars were moving away too fast around galaxies. For the galaxy to stay together - they should be flying apart at these speeds but, they aren't. They also noticed that the arms of spiral galaxies remain formed. In other words, the stars further out from the center don't move much slower than those closer in the arms of galaxies weren't just formation of stars, but pressure waves, where stars bunch up forming the arms, then spread apart again in between.

The only way to account for the observation was something called DM something that, so far, hasn't been detected. In order for the galaxies to remain as a structure, this DM has to make up about 95% percent of the mass so, what we see is only 5% of everything. There's a substance that makes up 95% of the universe that we simply don't know about it. DM is an undetected form of mass that emits little or no light but whose existence we infer from its gravitational influence [1].

It is a fundamental ingredient of our Universe and of structure formation, and yet its nature is elusive to astrophysical probes. Information on the nature and physical properties of the WIMP or neutralino (the leading candidate for a cosmological relevant DM) can be obtained by studying the astrophysical signals of their annihilation or decay.

Among the various electromagnetic signals, secondary electrons produced by neutralino annihilation generate synchrotron emission in the magnetized atmosphere of galaxy clusters and galaxies which could be observed as DM-induced radio emission centered on the DM halo.

A deep search for DM radio emission with SKA in local secondary electrons produced

by neutralino annihilation generate synchrotron emission in the magnetized atmosphere of galaxy clusters and galaxies which could be observed as DM-induced radio emission centered on the DM halo. A deep search for DM radio emission with SKA in local dwarf galaxies, galaxy regions with low star formation and galaxy clusters (with offset DM-baryonic distribution, like e.g. the Bullet cluster) can be very effective in constraining the neutralino mass, composition and annihilation cross-section.
For the case of a dwarf galaxy, the constraints on the DM annihilation cross-section obtainable with SKA1-MID will be at least a factor $\sim 10^3$ more stringent than the limits obtained by Fermi-LAT in the γ- rays. These limits scale with the value of the magnetic field and the SKA will have the capability to determine simultaneously both the magnetic field in the DM-dominated structures and the DM particle properties. The optimal frequency band for detecting the DM-induced radio emission is around$\sim 1GHz$, with the SKA1-MID Band 1 and 4 important to probe the synchrotron spectral curvature at low-ν (sensitive to DM compostion) and at high ν (sensitive to DM mass) [2].
The majority of the matter in the universe is still unidentified and under investigation by both direct and indirect means. What is the universe made of? One immediate answer which comes to mind is the universe is composed of all matter which we can see or which interact with light. Galaxies, stars, planets, humans and atoms are all made of electrons, protons, and neutrons. We call this ordinary matter which is visible. But is this the only component of the universe? We thought so for a long time until astronomers found that galaxies are rotating much faster than expected if they were made of ordinary matter only. This suggests that either the laws of gravity which describe many other processes very well should be modified or that the galaxy contains some other form of matter which we cannot see and haven't taken into account in our calculations.
Since we can measure the mass of the luminous part which consists of ordinary matter, we can also estimate the remaining mass which is invisible. This invisible mass component of the universe is called DM , and it is estimated to be more than 5 times the ordinary matter in the universe. DM is invisible because it does not emit or absorb light.
However it exerts gravitational force on ordinary matter which we can see it. Only 5% of the universe is made of ordinary matter such as atoms which make stars, planets, and us. The rest of the universe is dark and unknown, composed of dark matter and dark energy. Invisible dark matter makes up 27% of the universe, and we don't know its nature yet. Currently many experiments around the world are

searching for dark matter and we hope that in the near future we will solve the mystery of dark matter and understand its properties [12].

DM has become such an established paradigm in modern astro- explanation. Such blithe and widespread adoption of a cosmology in which an unknown matter plays the pivotal role has led some to become a little special about its existence. It is worth reminding ourselves, from time to time, of the strong and compelling evidence on which this paradigm actually stands. As it so happens, we will also pick up a good deal of information along the way about what properties DM must have [4].

Stars, galaxies, interstellar and intergalactic matter, radiation, magnetic field and cosmic rays are all the contents of the Universe. The question then naturally arises: What is the physical and kinematic nature of the Universe itself, when considered in its entirety? Cosmology is the science which attempts to give a satisfactory answer to this fundamental question regarding the understanding of the phenomena behind the cosm [8]. It is the study of the origin content, form, and time evolution of the Universe [6]. Cosmology aims to explain the origin and evolution of the entire contents of the Universe, the underlying physical processes, and there by to obtain a deeper understanding of the laws of physics assumed to hold throughout the Universe [7]. The basic requirement in formulating a theory of cosmology lies in truly knowing some of the basic facts about the Universe. These are, the shape (geometry) and size, the mass density and the total mass content, the age, the phase of its present dynamical behavior, and its chemical evolution with time. All this informations are very fundamental for the understanding of the nature of any object.

For any individual object or group of objects occupying any local region of space, this informations is not very difficult to acquire through experiments and theoretical postulates. But for the Universe as a whole, it is precisely these simple facts which pose great difficulties to be known. In fact, none of these basic facts has yet been known with any amount of definiteness when the Universe as a whole is concerned. Even the most powerful optical and radio telescopes available at present are unable to fathom the whole depth of the Universe. And whatever observations at large distances have been obtained, their true interpretation have very often eluded the scientists [8].

(DM) is an elusive form of matter that comprises 85.4%of the mass of the Universe (DM is 26.8%, luminous matter is 4.9%, and dark energy is 68.3%of thetotal mass-energy density). see figure1.1 Telescopes cannot observe it directly as it does not

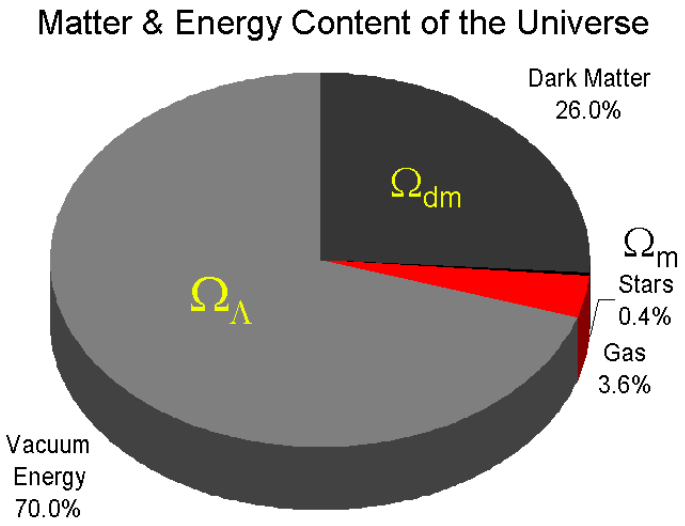

Figure 1.1: Matter and energy distribution in the universe today [12].

interact electromagnetically, but we can infer its presence from its gravitational effects on neighboring stars and galaxies. The most popular interpretation for DM is that it is aweakly interacting massive particle (WIMP). Competing theories include exotic particles ike axion-like particles (ALPs) or sterile neutrinos to account for the observed properties. Additionally theories such as modified Newtonian dynamics (MOND) or tensor-vector-scalar gravity (TeVeS) claim that gravitational anomalies in massive systems give rise to the perceived missing mass.

This work will focus on DM arising from WIMPs within the constraints of Lambda Cold Dark Matter (ΛCDM) cosmology, the accepted standard model for large-scale structure formation arising from non-relativistic DM. According to this current cosmological theory, in the early universe when the average temperature $\bar{T}$ exceeded the WIMP mass M_x(i.e., k_BT > $M_x \times$c^2) , where k_B is the Boltzmann constant and c is the speed of light a balance between the amount of WIMPs and photons that were spontaneously created or annihilated was established for a time. Once the temperature dropped below the equivalent mass-energy of the WIMP, the number of WIMPs began to fall exponentially according to:

$$N_x \propto (M_\chi T)^{\frac{3}{2}} e^{-\frac{M_\chi c^2}{k_B T}} \tag{1.1}$$

where $N_\chi$is the number density of WIMPs.

WIMPs are believed to be stable particles but also are their own antiparticle, hence they self-annihilate via the weak interaction into photons or other lighter particles

. Eventually the combination of the univers expansion and the annihilation of WIMPs shrank the WIMP number density to the point that further annihilations were unlikely to occur. As time went on, the mean free path for WIMP interactions extended out to the Hubble distance, thus fixing the interaction cross-section.
This remnant of the hot Universe called the thermal relic is present today and has an expected value:

$$< \sigma v >_{WIMP} \approx 3 \times 10^{-26} \frac{cm^3}{sec} \tag{1.2}$$

where $< \sigma v >_{WIMP}$ is the velocity-weighted cross-section for WIMP annihilation. This estimated value arising from the time-dependent Boltzmann equation has remained essentially unchanged since the early Universe due to the freeze-out process described above.
It also fits the measured DM density of several cosmological datasets including the Planck survey, baryon acoustic oscillations, and Type 1a supernovae lightcurves. The ratio of the DM density to the critical density of the Universe is given as:

$$\Omega_{DM} h^2 = 0.1123 \pm 0.035 \tag{1.3}$$

where Ω_{DM} is the DM density and h is the dimensionless Hubble parameter at the current epoch (z = 0) in units of $100 kms^{-1} Mpc^{-1}$.
Alternatively, theories for the decay of DM into other Standard Model particles have been proposed with the decay time being a free parameter. At Earth (8.33 kpc from the center of the Milky Way) the DM density has been estimated to be $0.3 \pm 0.1 GeV/cm^3$. The DM takes the form of a large spherical halo around the Milky Way galaxy. DM must be present in this concentration for the Solar System and other stars to traverse the galaxy in orbits that satisfy the Jeans equation and other best-fit halo models. The evolution of the halo and substructures traces the hierarchical development of the galaxy.
The standard picture from numerical simulations is that smaller clumps of DM coalesed with the galaxy's halo over megayears growing in size similar to the way smaller satellite galaxies merged with the galaxy's disk. While DM does clump under the influence of self-gravity, it should not virialize or form a disk because DM is believed to be nearly collisionless. It does not have to transfer and lose angular momentum the way interacting gas and dust do during collapse [10]. On large scales, the Universe shows a wealth of structure: galaxies are gathered into clusters, clusters are part of super-clusters, and super-clusters are arranged into large-scale sheets, filaments and voids. Presumably, the pattern of galactic superstructure reflects the history of gravitational clustering of matter since the

Big Bang.
If DM was present during structure formation, it should have influenced the pattern of large-scale structure we see today. Large-scale cosmological $'N-body'$ simulations demonstrate that, the observed largescale structure of luminous matter could only have been formed in the presence of a substantial amount of dark matter. Furthermore, the bulk of dark matter must be both cold and non-dissipative for the correct structures to be produced. $'Cold'$ in this context means that it moves very non-relativistically, and so has a short free-streaming length (less than the size of a gas cloud undergoing gravitational collapse, for example). Being cold means that the dark matter can gather gravitationally on small scales and so seed galaxy formation, but being non-dissipative prevents it from cooling and collapsing with the luminous matter, which would produce larger and more abundant galactic disks than are observed. Hot (highly relativistic) and warm (borderline relativistic) dark matter could still make up a fraction of the total dark matter, though just how large a fraction depends critically upon how warm that fraction is.
Large-scale galaxy surveys not only provide information as to the amount and pattern of structure present in the Universe, but also a handle on the total mass contained within it. To a first approximation, the characteristic size of baryonic density perturbations which can survive until matter-radiation equality (and therefore collapse to form galaxies and clusters) is set by the mean density of baryons in the Universe smaller perturbations are destroyed by radiative and neutrino damping, larger ones fragment.
In the presence of an additional matter component which gravitates but does not couple radiatively to the baryons, the power spectrum of pertur-bations which ultimately survive to form galaxies is modified by the enhanced gravitational clustering. The resulting large-scale galaxy power spectrum is thus strongly dependent upon the total matter density of the Universe, and weakly dependent upon the fraction of matter contained in baryons. Recent surveys indicate a total matter (i.e. dark plus luminous matter) density of $\Omega_m \equiv \rho_m/\rho_c \approx 0.29$ [11] , where ρ_c is the critical density required to close the Universe.

These facts provide the basic motivations for our study, which is generally aimed to study various (DM) annihilation channels in radio frequency in order to explore the possibility to interpret the still unknown origin of radio emission in a coma like simulated galaxy clusters and more specifically aimed to

1. Study the distribution of DM in Coma like galaxy cluster (area in the universe thought to be dominated by DM)

2. Produce radio emission maps and graphs for diffrent annihilation channels and DM masses.

Thus, it is clear that our work has two sides: On one hand, we are searching for source of realtivistic electrons which are responsible for the diffused radio emission and on the other hand we are making an indirect detection of DM within the galaxy clusters.
The break down of this thesis is as follows: In chapter one, we present a definition of DM, its properties as well as evidences for DM and objective of the study. We close chapter one answering questions such as: what is the identity of DM and how it could be detected. In chapter two radio emission from DM annihilation processes in galaxy Clusters and different models for the possible sources of the relativistic electrons which are responsible for the radio emission from DM annihilation processes are broadly discussed. Where as in the third chapter we present the modeling for the radio emission with the proper mathematical formulation of the magnetic field strength, the electron equilibrium spectra, the local emissivity and ultimately the flux. We conclude chapter three by introducing the data sources and the simulation techniques followed by the data analysis. In chapter four the results (radio emission maps, tables and graphs) obtained from the simulation and their elaborated discussions will be presented. At the end in chapter five, I will give conclusion of my own work.

1.1 Evidence for Dark Matter

The Swiss astronomer Fritz Zwicky was the first to surmise the presence of DM which he termed dunkle materie. He noticed something unusual from galaxy rotaion curves, gravtionallensing, the Cosmic Microwave Background Radiation etc. we will discuss each of them one by one.

1.2 Gravtional lensing

A gravitational lensing is a distribution of matter between a distant light source and an observer, that is capable of bending the light from the source as the light travels towards the observer. If the (light) source, the massive lensing object, and

the observer lie in a straight line, the original light source will appear as a ring around the massive lensing object. If there is any misalignment, the observer will see an arc segment instead. More commonly, where the lensing mass is complex

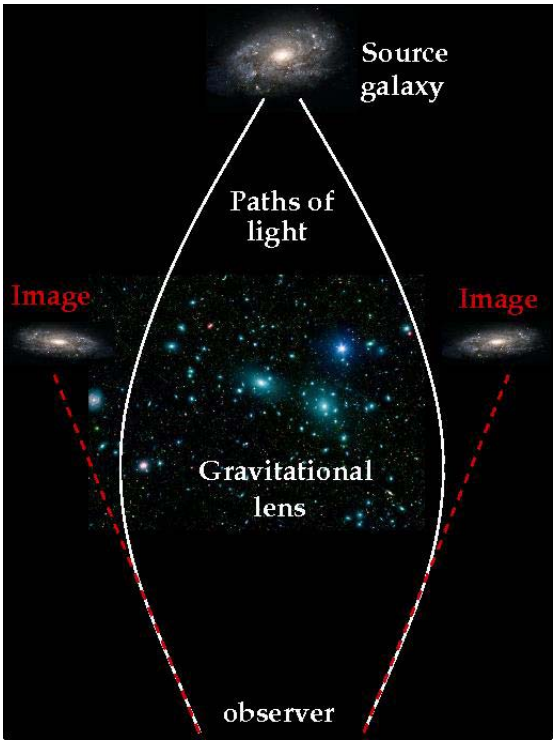

Figure 1.2: Gravitational lensing concept [12].

(such as a galaxy group or cluster) and does not cause a spherical distortion of space time, the source will resemble partial arcs scattered around the lens. The observer may then see multiple distorted images of the same source; the number and shape of these depending upon the relative positions of the source, lens, and observer, and the shape of the gravitational well of the lensing object. There are three types of lensing. Strong gravitational lensing is a gravitational lensing effect that is strong enough to produce multiple images, arcs, or even Einstein rings. Generally, the strong lensing effect requires the projected lens mass density greater than the critical density.

For point-like background sources, there will be multiple images; for extended background emissions, there can be arcs or rings. Weak gravitational lensing is thus an intrinsically statistical measurement, but it provides a way to measure the masses of astronomical objects without requiring assumptions about their-composition or dynamical state. It is used, where the distortions of background sources are much smaller and can only be detected by analyzing large numbers of

sources in a statistical way to find coherent distortions of only a few percent.
The lensing shows up statistically as a preferred stretching of the background objects perpendicular to the direction to the centre of the lens. By measuring the shapes and orientations of large numbers of distant galaxies, their orientations can be averaged to measure the shear of the lensing field in any region. This, in turn, can be used to reconstruct the mass distribution in the area: in particular, the background distribution of DM can be reconstructed. Since galaxies are intrinsically elliptical and the weak gravitational lensing signal is small, a very large number of galaxies must be used in these surveys.

Gravitational micro-lensing is an astronomical phenomenon due to the gravitational lens effect. It can be used to detect objects that range from the mass of a planet to the mass of a star, regardless of the light they emit. Typically, astronomers can only detect bright objects that emit much light (stars) or large objects that block background light (clouds of gas and dust). These objects make up only a minor portion of the mass of a galaxy. Micro-lensing allows the stufixsen1996cosmicdy of objects that emit little or no light. Since microlens-ing observations do not rely on radiation received from the lens object, this effect therefore allows astronomers to study massive objects no matter how faint. It is thus an ideal technique to study the galactic population of such faint or dark objects as brown dwarfs, red dwarfs, planets, white dwarfs, neutron stars, black holes, and massive compact halo objects. Moreover, the micro-lensing effect is wavelength-independent, allowing use of distant source objects that emit any kind of electromagnetic radiation. Micro-lensing by an isolated object can be detected by astronomers. Since then, micro-lensing has been to constrain the nature of the DM. When light is coming from a distant bright source such as a star, it has been formed a partial arc around DM, these mechanism helped us to study the property and nature of DM. we can analyze the distortion and predict the stastical distribution and amount of DM in the galctic cluster and its subhalos [13].

1.3 The Cosmic Microwave Background Radiation

Most of the photons of light produced by various sources in the Universe which are collectively detected on earth by various instruments or telescopes are not from stars, but from the Cosmic Microwave Background (CMB). In 1965 Penzias and Wilson detected some radiation at a microwave wavelength which was coming from

all points in the sky.
Initially, having failed to avoid this radiation appearing in the telescope they thought it due to some kind of defect in the instrument or faulty measurement. However, when they learnt that there has been theoretical predictions of relic radiation that should be left over from the Big Bang, it became a discover [14].

CMB radiation is a relic radiation that is left over from the early Universe which is predicted in the $"HotBigBang"$ model. It is deduced that if the Universe started from a hot and dense state, it should now be filled with radiation in the microwave range due to redshift. With an experimental measurement made outside the atmosphere of the Earth, the CMB spectrum was first measured accurately over a wide range of wavelengths by the COsmic Background Explorer (COBE) [15].

It showed that the CMB has nearly perfect thermal black body spectrum at a temperature of 2.7277 K with a close resemblance to isotropy with tiny variations of 30 micro kelvins in temperature across the sky[16]. The expected temperature fluctuations of anisotropy in the CMB assuming weakly interacting dark matter components are in the order of $5\delta_T T \simeq 10$ [15].

This value falls in the regime of micro kelvins which were finally detected at the same level by COBE in 1992 . Further substantially improved mea- surements has led to a conclusion that the structures formed in the Universe that we observe today are the results of these anisotropies where the attractive force of gravity acted upon them [16].

1.4 Rotation curve of a galaxy

The Swiss astronomer Fritz Zwicky was the first to point out the presence of DM which he termed dunkle materie. He noticed something unusual about the movement of galaxies within the Coma cluster (Abell 1656). He applied the time-averaged virial theorem: $\bar{T} + \bar{\Omega} = 0$ where $\bar{T}$ is the average kinetic energy of the galaxies in the cluster and $\bar{\Omega}$ is the average gravitational potential energy of the cluster. The value of $\bar{\Omega}$ he arrived at by summing up the potentials of the galaxies was ~ 400 times smaller than the measured kinetic energy required to keep the system in equilibrium.

The gravitational influence of the luminous matter alone was unable to account for the rapid motions of the individual galaxies. The result, that DM is present in much larger quantities than luminous matter, surprised him greatly . While later studies of the Coma cluster revealed a slightly lower mass-to-light ratio (M/L) of ~ 350 (from improved mass resolution), the critical importance of his discovery continues to shape the face of modern astrophysics.

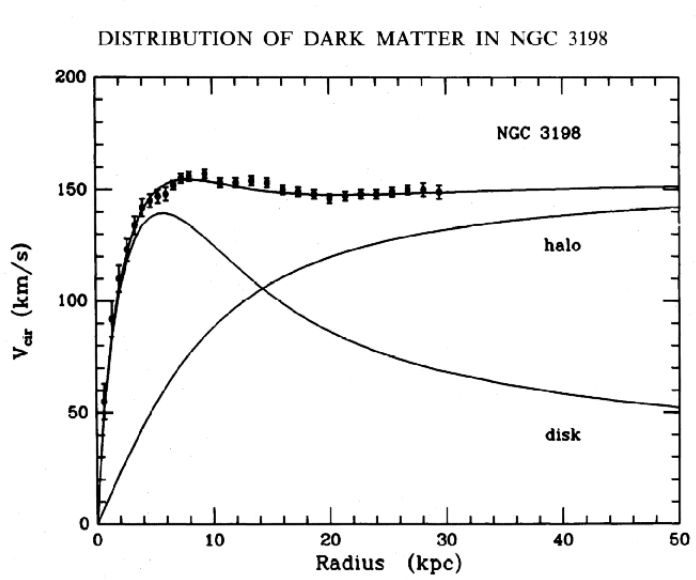

Figure 1.3: NGC 3198 galactic rotation profile (credit: T. S. van Albada). [12].

The velocity of stars orbiting around the center of a galaxy should fall inversely as the square root of the radial distance if bound by the gravity of the luminous matter that is mostly concentrated in the bulge of the galactic disk. Keplerian orbital dynamics for stars outside of the bulge gives:

$$F_{cent} = \frac{GMm}{R^2} = \frac{mv^2}{R}, v = \sqrt{\frac{GM}{R}} \tag{1.4}$$

where F_{cent} is the centripetal force, G is the gravitational constant, M is the mass of the bulge, m is the mass of the star, v is the orbital velocity, and R is the radius of orbit. Within the bulge, however, the velocity increases proportionally to R.

In the 1970's Vera Rubin made measurements of local galaxies with a high-resolution spectrograph. Her observations indicated that the radial velocity curves stay flat out to large radii. Figure 1.3 points out the discrepancy between the observed and expected radial velocity curve for the galaxy NGC 3198. The missing mass is

believed to lie in a spherical halo of dark matter around the galaxy. The points with error bars are the observed radial velocities of stars in the galaxy. The three curves are model predictions of the relative gravitational strengths on the radial velocity. The halo curve (DM) plus the disk (galactic bulge) curve yield the combined model prediction [12].

1.5 Dark matter candidates

From observational evidences accumulated so far on the existence of DM a list of its properties can be inferred. There are three basic properties that DM candidates must have:

i) DM is dissipation less, which means it involves only in a very weak electromagnetic interaction. DM is nearly collision-less i.e., the interaction cross-section between DM and baryonic matter for densities found in DM halos is so small to be considered negligible. This also means that its particles are only gravitationally bound to one another and travel unimpeded in orbits in the halos with a broad spectrum of eccentricities. ii) DM is cold, which means that they move at non-relativistic speed as they enter matter dominated aera and to cluster effectively and produce the observed intricate structures we observe today; ii) DM is stable, which means that its life time must be comparable to or greater than the age of the Universe. Moreover DM behaves classically to be confined on galaxy scales through attractive gravitational interactions; and as a fluid on galaxy scales as its discreteness is not proved yet.

Thus it goes without saying that these properties of DM which are known so far are to be used as a reference point (to compare with) in the search for the right candidates. Behave as a perfect fluid on large scales, meaning that the granularity of the dark matter is sufficiently fine not to have been directly detected yet through various effects [17].

1.6 Baryonic dark matter

By baryonic matter, we mean ordinary matter composed of protons, neutrons and electrons. Certain forms of baryonic matter are very difficult to detect because they are very weak emitters of electromagnetic radiation. Examples of such weak emitters are brown dwarf stars with masses $M \leq 0.08 M_{\odot}$ in wich the central temperatures are not hot enough to burn hydrogen into helium. Although brown dwarfs are estimated to be about twice as common as stars with masses $M \geq 0.08 M_{\odot}$, they contribute very little to the mass density in baryonic matter as compared with normal stars because of their low masses. The consensus of opinion is that brown dwarfs could only make a very small contribution to the DM.

Black holes are another possibility for the DM. The super-massive black holes in the nuclei of galaxies have masses which are typically only about 0.1 percent of the mass of the bulges of their host galaxies and so they contribute negligibly to the mass density of the Universe. There might, however, be an invisible intergalactic population of massive black holes. Limits to the number density of black holes can be set in certain mass ranges from studies of the numbers of gravitationally lensed images observed in large samples of extragalactic radio sources. The upper limit to the cosmological mass density of these black holes corresponded to less than 1 percent of the critical cosmological density [18].

An impressive approach to setting limits to the contribution which discrete low mass objects, known as MAssive Compact Halo Objects, or MACHOs, could make to the DM in the halo of our own Galaxy, has been the search for gravitational microlensing signatures of such objects as they pass in front of background stars. The MACHOs include low mass stars, white dwarfs, brown dwarfs, planets and black holes. These lensing events are very rare and so very large numbers of background stars have to be monitored. This technique is sensitive to MACHOs with a very wide range of masses, from 10^{-7} to $100 M_{\odot}$

.

In addtion the expected light curve of such gravitational lensing events has a characteristic light curve which is independent of wavelength. The time-scale of the brightening is roughly the time it takes the MACHO to cross the Einstein radius of the dark deflector. The first example of such a microlensing event was

discovered in October 1993, the mass of the invisible lensing object being estimated to lie in the range $0.03 < M < 0.5M_{\odot}$ [19]. By the end of the MACHO project, 13 definite and four possible events were observed in the direction of the Large Magellanic Cloud, significantly greater than the 2 up to 4 detections expected from known types of star. The best statistical estimates suggest that the mean mass of these MACHOs is between 0.15 and $0.9M_{\odot}$

. The statistics are consistent with MACHOs making up about 20% of the necessary halo mass. Somewhat fewer microlensing events were detected in the EROS project which found that less than 25% of the mass of the standard DM halo could consist of dark objects with masses in the range 2×10^{-7} to $1M_{\odot}$ at the 95% confidence level. The consensus view is that MACHOs alone cannot account for all the DM in the halo of our Galaxy and so some form of non-baryonic matter must make up the difference [20].

1.7 Non-baryonic dark matter

Non-baryonic dark matter are divided into two, hot dark matter (HDM) and cold dark matter (CDM), based on the typical velocities of the particles making up this matter. baryonic BDM, HDM, and CDM all have a different effect on structure formation in the universe. Structure formation refers to how the originally almost homogeneously distributed matter formed galaxies and galaxy clusters under the pull of gravity. If dark matter particles are called HDM, they decouple while still relativistic, so that they retain a large number density, requiring their masses to be small, less than 100 eV, so that they would not contribute much more than the critical density to the universe. Because of these small masses, their thermal velocities are large when structure formation begins, making it difficult to trap them in potential wells of the forming structures. Cold dark matter Non-baryonic matter which is non-relativistic at the epoch of radiation- matter equality. This component, known as cold dark matter (CDM), is still the leading contender for the non-baryonic dark matter of the Universe, and has been remarkably successful in explaining the observed large scale structures of the Universe. For a particle species in thermal equilibrium in the early Universe, the particle mass must be >1keV in order for it to qualify as CDM. At masses of 1keV, it would instead behave as HDM. Current cosmological observations constrain the non-baryonic matter component of the Universe to have an equation of state with $1.5 \times 10^{-6} < w < 1.13 \times 10^{-6}$ [21], i.e. in excellent agreement with the CDM hypothesis. The currently

favored cosmology (with $\Omega_m \sim 0.3, \Omega_\lambda \sim 0.7$) in which most of the matter is assumed to be CDM. Apart from non-relativistic velocities (dynamical $"coldness"$), a number of additional dark matter properties are usually assumed in the CDM scenario. The CDM particles are also assumed to:

1 be collision less, meaning that they interact through gravity only and have no other significant self-interactions; 2 be dissipation less, meaning they cannot cool by radiating photons (as opposed to normal baryonic matter); 3 be long-lived, meaning that their lifetimes must be comparable to or longer than the present age of the Universe; behave as a perfect fluid on large scales, meaning that the granularity of the dark matter is sufficiently fine not to have been directly detected yet through various effects [21].

1.8 Weakly interacting massive particles (WIMPS)

WIMPS: Weakly interacting massive particles (WIMPS) are smaller than atoms. They have mass, but their interactions are so weak that they pass right through ordinary matter. Since each a WIMP has only a small amount of mass, there needs to be a large number of them to make up the bulk of DM. That means that millions of WIMPs are passing through ordinary matter such as the Earth and the Sun every few seconds. Stable weakly interacting massive particles (WIMPs) are attractive cold DM candidates.
The WIMPs in our galaxy halo can be gravitationally trapped and accumulated by the Sun and the Earth. They can annihilate into weak bosons and heavy quarks which subsequently decay into neutrinos. Because of their lack of strong interaction with normal matter and lack of interaction through electromagnetism, they would appear dark in current telescopes, unless they happen to decay or annihilate into photons. Although there are no known particles within the standard model of particle physics which correspond to WIMPs, supersymmetric extensions contain a host of potential WIMP candidates. WIMPs have mass in the range m weak = 10GeV to 1T eV and tree-level interactions with W and Z gauge bosons, but not with gluons or photons. WIMPs are the most studied DM candidates, as they are found in many particle physics theories, naturally have the correct relic density, and may be detected in many ways.

WIMPs gravitationally captured by scattering interactions with nucleons in the Sun and Earth could then annihilate and produce a detectable neutrino flux. Once

captured, a WIMP continues to scatter, losing energy and sinking to the core of the Sun or Earth; a large abundance of WIMPs can accumulate through this mechanism. If a WIMP is stable, it is naturally produced with a relic density consistent with that required of DM. DM may be produced in a simple and predictive manner as a thermal relic of the Big Bang [22]. Initially the early Universe is dense and hot, and all particles are in thermal equilibrium. The Universe then cools to temperatures T below the dark matter exists as particles of mass M_x and the number of DM particles becomes Boltzmann suppressed, dropping exponentially as $e^{(-m_x/T)}$. The number of DM particles would drop to zero, except that, in addition to cooling, the Universe is also expanding . In the third stage, the Universe expand and becomes so large and the gas of DM particles becomes so dilute that they cannot find each other to annihilate. The DM particles then freeze out, with their number asymptotically approaching a constant to their thermal relic density. Note that freeze out, also known as chemical decoupling, is distinct from kinetic decoupling; after thermal freeze out, interactions that change the number of DM particles become negligible, but interactions that mediate energy exchange between DM and other particles may remain efficient. This process is described quantitatively by the Boltzmann equation $dn/dt = -3H_n - < \sigma_{AV} > (n^2 - n_{eq}^2)$ where n is the number density of the DM particle X, H is the Hubble parameter, $< \sigma_{AV} >$ is the thermally averaged annihilation cross section, and n_{eq} is the DM number density in thermal equilibrium. On the right-hand side of the above equation, the first term accounts for dilution from expansion. The n_2 term arises from processes $XX \rightarrow SMSM$ that destroy X particles, where SM denotes standerd model particles, and then_{2eq} term arises from the reverse process $SMSM \rightarrow XX$, which creates X particles . The thermal relic density is determined by solving the Boltzmann equation numerically. Defining freeze out to be the time when $< \sigma_{AV} >= H$ we have

$$n_f \sim (m_x T_f)^{3/2} (e^{-m_x/T_f}) n_f \sim (T_f^2 / M_{p1} < \sigma_{AV}) >) \tag{1.5}$$

where the subscripts f denote quantities at freeze out. The ratio $X_f = m_x/T_f$ appears in the exponential. It is, therefore, highly insensitive to the DM's properties and maybe considered a constant; a typical value is $x_f = 20$. The thermal relic density is, then,

$$\Omega_x = m_x n_o / \rho_c \Omega_x = (m_x T_o^3 / \rho_c)(n_0 / T_0^3) \Omega_x \sim (m_x T_o^3 / \rho\_ c M_{p1}) < \sigma_{AV} > \tag{1.6}$$

Where ρ_c is the critical density and the subscripts 0 denote present day quantities. We see that the thermal relic density is insensitive to the DM mass m_x and inversely

proportional to the annihilation cross section $< \sigma_{AV} >$. The annihilation cross section can be written as

$< \sigma_{AV} >= k(g^4_{weak}/16\Pi^2 m^2_x$

The constant$g_{weak} \sim 0.65$ is the weak interaction gauge coupling, and k parameterizes deviations from this estimate. With this parametrization, given a choice of k, the relic density is determined as a function of m_x . We see that a particle that makes up all of DM is predicted to have mass in the range $m_x \sim 100GeV - 1TeV$; a particle that makes up 10%of DM has mass $m_x \sim 30GeV - 300GeV$. This is the WIMP miracle: weak-scale particles make excellent DM candidates[22].

1.9 Massive Astrophysical Compact Halo Objects (MACHOs)

The MACHOs (Massive Astrophysical Compact Halo Objects) are large astrophysical objects which for some reason do not emit much light with masses substantially larger than those of WIMPs, objects like failed stars in mind, many non-baryonic candidates can in fact behave as MACHOs. Therefore, contrary to a wide-spread misconception in the astronomical community, the MACHO populations that can be probed through micro lensing effects are not necessarily subject to constraints on the baryonic mass fraction of the Universe, and can in principle constitute all of the dark matter (although current constraints make this seem unlikely).

Certain kinds of MACHOs could further more have a sufficiently small interaction with the baryonic content of the Universe to effectively behave as CDM. It should also be noted that despite the meaning of the acronym, MACHOs do not associated with dark matter halos (but rather with low-density regions like filaments) are nowadays also being considered. Of course, not all dark matter candidates fall within the definitions of WIMPs and MACHOs. Some of those described in the following are neither, while others are both [23].

1.10 The annular modulation signal

If the DM halo of the Milky Way is in the form of WIMPs, the Earth should experience a WIMP wind of such particles as it moves through the halo due to its orbit around the Sun and the orbit of the Sun around the centre of the Galaxy.

These WIMPs can in principle be detected through rare elastic scatterings off nuclei in a sufficiently sensitive detector on Earth. The scatterings may however easily drown in a background of other effects picked up by the detector. To evade this problem, one exploits the fact that the strength of the WIMP wind should display a seasonal variation with a well-defined period and phase. In June, the velocity of the Earth around the Sun is added to the velocity of the Sun around the Milky Way, it is giving maximal WIMP flux on Earth, whereas in December these two velocities act in the opposite directions, which is giving minimal WIMP flux. Because of this effect, the events induced by WIMPs should show an annular modulation [23].

1.11 Standard model particles (SMP)

The particles of the SM are divided into three categories:
a) Spin 1/2 Fermions: These matter particles include six flavors of quarks (up, down, charm, strange, bottom, and top), three flavors of charged leptons (electrons, muons, and taus), and three favors of neutral leptons (the electron, muon, and tau neutrinos).
b) Spin 1 Gauge Bosons: These force carrying particles include the photon, which mediates electromagnetism; eight gluons g, which mediate the strong force; and the W and Z gauge bosons, which mediate the weak interactions. The photon and gluons are mass less, but the W and Z have masses 80 GeV and 91 GeV, respectively.

c) Spin 0 Higgs Boson: The SM Higgs particle is a spin 0 boson. Although the Higgs boson has not yet been discovered, its mass is constrained by a variety of collider results. Assuming the SM, null results from direct searches at the LEP e^+e^- collider Require $m_h > 114.4GeV$. Given this constraint, precision measurements of electroweak observables at LEP require $m_h < 186GeV$'

In addition, the Tev electron protn-protn collider, currently running, excludes the region $162GeV < m_h < 166GeV$. These bounds may be relaxed in extensions of the SM, but even in such theories, main general arguments require m_h not yet been 1 TeV. The photon and gluon are mass less. The Higgs boson has discovered, its mass has been taken in the allowed range $114.4GeV < m_h < 186GeV$. None of these SM particles is a good dark matter candidate. Most of he matter particles are

unstable, with lifetimes far shorter than the age of the Universe. The remaining particles are the six lightest: the electron, the up and down quarks, which may form stable protons and neutrons in nuclei, and the three neutrinos. Electrons may contribut significantly to dark matter only if they are neutralized through binding with protons, but protons (and neutrons) contribute to the baryonic energy density Q_B , which is too small to be all of dark matter.

In addition, current upper bounds on neutrino masses from particle physics and cosmology imply that the neutrino relic density $Q_v \sim \Sigma_i(m_i/47ev) \leq 0.012$. The evidence for dark matter therefore requires particles beyond the SM[22].

1.12 Supper symmetry particles

Super symmetry is a high-energy extension of the standard model of particle physics, in which symmetry between bosons (particles with integer spin) and fermions (particles with half-integer spin) is assumed to exist. In this picture, every standard fermion is accompanied by a bosonic super particle, and every standard boson by a fermionic one. For the super partners of standard fermions, an "s" is added as a prefix to the name (i.e electron becomes selectron), while for the super partners of standard bosons, the last syllable of the name is replaced by "ino" (i.e. photon becomes photino).

Hence a zoo of new particles is predicted to exist (e.g. neutrinos, gluinos, quarks), and may have been created in great numbers in the early universe. A super symmetricparticle cannot decay into normal particles only, which means that the lightest super symmetric particle must be stable. This would make it a good candidate for the non-baryonic dark matter. The super symmetry generating the most articles is the neutralino, but other options such as the axino (the super symmetric partner to the axion) and the gravitino are also viable options. If super symmetric particles exist, they may be detected in upcoming high energy particle colliders like the Large Hadron Collider at CERN provided that their mass is lower than a few hundred GeV [24].

1.13 DM Detection Searches

One of the preferred candidates of dark matter is a particle which interacts weakly with ordinary matter. Millions of such dark matter particles could be passing through Earth each second, but because of their weak interactions they are very hard to detect. There are three different complementary ways to detect dark matter [10].

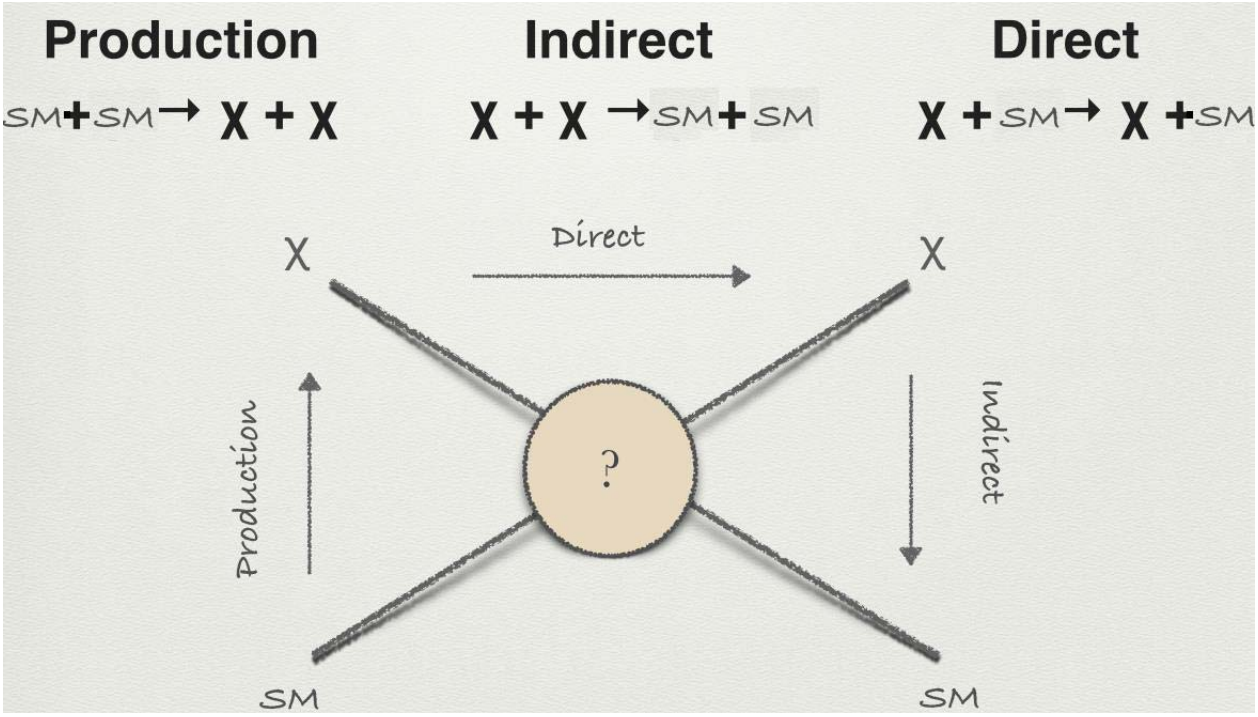

Figure 1.4: The three DM detecation methods [10].

1.14 Direct detection of DM

There are many experiments deep underground searching for the effect of a dark matter particle passing through the detector. The DM particle can collide with an atom in the detector and produce heat or light which can be measured [10].

1.15 Indirect detection of DM

Indirect detection of DM is the technique of observing the radiation produced in DM annihilations. The flux of such radiation is proportional to the annihilation rate, which in turn depends on the square of the DM density, $\Gamma_A \propto \rho_{DM}^2$. Therefore,

the "natural" places to look at, when searching for significant fluxes, are the regions where large DM densities accumulate. This regions are referred as amplifiers. Dense regions of the galactic halo, such as the galactic center, may be excellent amplifiers for the purposes of detecting gamma rays or neutrinos.
Annihilation products which are charged move under the influence of magnetic fields making it impossible to consider point sources of such radiation. Despite this, observations of cosmic positrons and anti-protons can be valuable tools in searching for particle [10].

1.16 Production in laboratory(Detection from particle colliders)

Another way to detect dark matter is to produce it in the laboratory. Experiments in the Large Hadron Collider (LHC) at CERN will look for dark matter produced after protons coming from opposite directions collide at high energies and speeds. Direct detection is currently the most promising method to search for dark matter, and there are several direct dark matter experiments running all over the world. These detectors are built deep underground to avoid the background from cosmic rays. Cosmic rays which are constantly coming towards the Earth collide with the upper atmosphere and create a shower of particles reaching the surface of the Earth. Thus it is important to built the dark matter detectors deep underground to avoid such backgrounds. So far many experiments which use different materials in their detectors and different detection techniques have found hints for a dark matter particle.
Their hints are not completely consistent with each other, and also are in disagreement with results from several other experiments which have not found any signals. The nature of dark matter is still unknown, but with the current level of sensitivity reached by the experiments, we are hopeful to detect dark matter soon and shed light on this dark mystery [10].

1.17 Short Summary of the chapter

In this chapter we paved a way to the main topic which is dark matter (DM). we start by setting two fundamental principles of cosmology, i.e. the homogeneity and isotropy of our Universe. This principles make it easy to come up with different

models of the Universe. The matter energy budget of the Universe tell us that about 95% of the Universe is invisible of which DM takes 26% . Astronomical observations makes us certain about the existence of this DM whose influence is seen on the visible matter. And finally, we have introduced the possible DM candidates and indicated the three detection mechanisms.

CHAPTER 2

Diffused radio Emission from DM Annihilation Processes in Galaxy Clusters

2.1 Introduction

Clusters of galaxies are the largest gravitationally bound systems in the Universe, with typical masses of about $10^{15} M_{\odot}$

, and volumes of about $100 Mpc^3$.

Most of gravitating matter in any cluster is in the form of DM. Some of the luminous matter is in galaxies $\sim (3\% - 5\%)$, the rest is in diffuse hot gas $\sim (15\% - 17\%)$. This thermal plasma, consisting of particles of energies of several keV, is commonly referred to as Intracluster Medium (ICM). Clusters are formed by hierarchical structure formation processes.

In this scenario, smaller units (galaxies, groups and small clusters) formed first and merged under gravitational pull to larger and larger units in the course of time. Cluster mergers are the mechanism by which clusters are assembled.

Denser regions form a filamentary structure in the Universe, and clusters are formed within filaments, often at their intersection, by a combination of large and small mergers. Major cluster mergers are among the most energetic events in the Universe since the Big Bang. During mergers, shocks are driven into the ICM, with the subsequent injection of turbulence. The merger activity, which has characterized much of the history of the Universe, appears to be continuing at the present time and explains the relative abundance of substructure and temperature gradients detected in clusters of galaxies by optical and X-ray observations.

There are a number of observational results obtained recently related to the diffuse radio sources from galaxy clusters. In this chapter we will discuss about this diffuse and extended radio emission from galaxy clusters and we present the approach used by three models to explain the possible sources for the relativistic electrons which are responsible for this extended emission [25].

2.2 Radio emissions in galaxy clusters

Galaxy clusters are characterized by emission in the radio band among others. Obvious radio sources are the individual galaxies, whose emission has been observed in recent decades with sensitive radio telescopes. It often extends well beyond the galaxy optical boundaries, out to hundreds of kpc, and hence it is expected that the radio emitting regions interact with the ICM. This interaction is indeed observed in tailed radio galaxies, and radio sources filling X-ray cavities at the centre of cool core clusters [25].

More puzzling are diffuse extended radio sources, which cannot be obviously ascribed to individual galaxies, but are instead associated with the ICM. This radio emission represents a striking feature of clusters, since it demonstrates that the thermal ICM plasma is mixed with non-thermal components. Such components are large scale magnetic fields with a population of relativistic electrons in the cluster volume.

In recent years, there has been growing evidence for the existence of cluster large scale diffuse radio sources, of synchrotron origin, which have no optical counterpart and no obvious connection to the cluster galaxies, and are therefore associated with the ICM. The first diffuse radio source detected in a cluster of galaxies is the giant radio halo at the center of the Coma cluster. Several years later, extended diffuse emission was also detected at the periphery of the Coma cluster and at the center of the Perseus cluster.
Nowadays, diffuse radio emission with surface brightness down to $0.1\mu arcsec^{-2}$ at 1.4 GHz is known in about 80 clusters, under several cluster evolutionary conditions (merging and relaxed clusters), at different cluster locations (center, periphery, intermediate distance), and on very different size scales from 100 kpc to > Mpc [25].
Galaxy cluster regions which show diffuse synchrotron emission are in general divided into radio halos and radio relics see Fig. 2.1. Radio halos and relics are faint (μ J yarcsec^{-2} 1.4 GHz) sources extended on Mpc scales , located at the center and in the outskirts of about 100 merging galaxy clusters, respectively.
The study of radio halos and relics is of paramount importance to shed light on the history and physical properties of galaxy clusters, and to clarify the role of non-thermal components associated to the ICM. Their nature reveals very weak large-scale magnetic fields, with central strengths $\sim \mu G$, fluctuation scales of up

to several hundreds of kpc, and rarefied, very energetic populations of relativistic electrons spread across the cluster volume [25].

There are two observables about the diffused radio spectrum i.e, the integrated

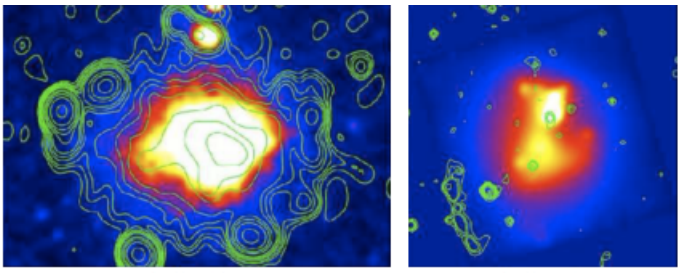

Figure 2.1: Image of radio halos (left) and radio relics (right) showing the extended diffuse radio emission at the cluster center and periphery, respectively

Image adapted from [27].

radio spectra and the spatial variation of the spectral index. The integrated radio spectra of halo sources are still poorly known. The difficulty of spectral studies are that i) only in a few cases the spectrum is obtained with more than three flux density measurements at different frequencies, ii) for most sources the highest available frequency is 1.4 GHz, therefore it is difficult to determine the presence of a spectral steepening, crucial to discriminate between different reacceleration models.

The best studied integrated radio spectrum is that of the Coma cluster where clear evidence of a high frequency steepening is present (see Fig. 2.2) for a detailed discussion. A powerful tool to understand the physical properties of radio halos is the spectral index map. It reflects the variation of the shape of the electron energy distribution (see Eq. 2.2) and of the magnetic field in which they emit. Measurment of the spatial distribution of spectral index of the radio emission from the DM annihilation within the galaxy cluster provides a valuable physical information for understanding the structure of the DM in the cluster. Mapping the spatial distribution of spectral index represents a powerfull tool to study the properies of the relativistic electrons and the magnetic field in which they emit and investigate the connection between the electron energy distribution and the ICM . The first spectral index map of a radio halo was obtained for the Coma cluster. The spectral distribution is smooth with a steepening from the center to the peripheral regions, where the spectral index is $\alpha \sim 2$. The spectral index images of giant radio halos in A665 and A2163, with an angular resolution $\sim 1'$, show flattening and patches,

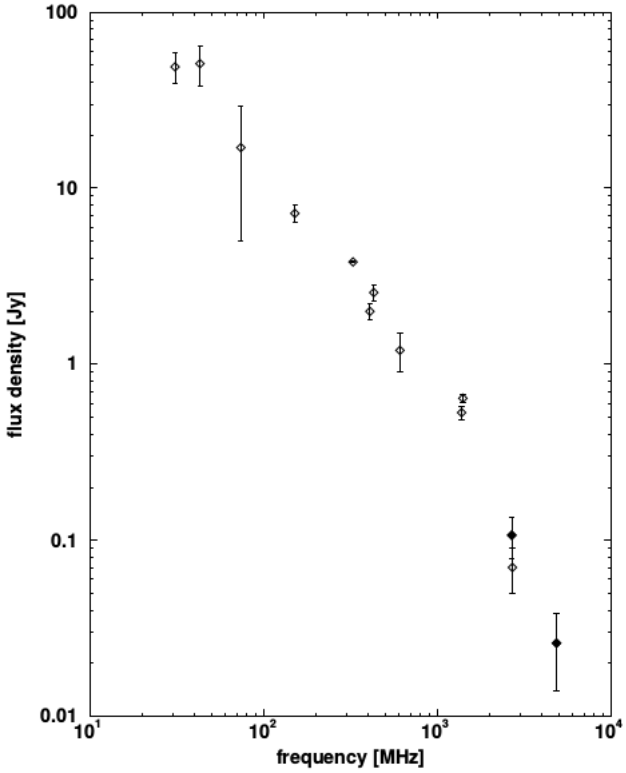

Figure 2.2: Integrated radio continuum spectrum of the diffuse radio halo source Coma C. The filled dots represent new observations made by (Thierbach et al., 2003)

[28].

and radial steepening in the undisturbed cluster regions [25]. Spectral variations are likely to reflect the energy losses/gains of the radiating electrons. The spectral index is given by the formula:

α=$ln(F_1/F_2)/ln(\nu_1/\nu_2)$,

Where F_1 and F_2 are flux values at frequency v_1 and v_2 respectively. The spectral index can be used to determine the electron energy distribution given by: $N(E)d(E) = N_oE^{-\delta}$ where the injection spectral index, δ of the electron energy distribution is related to the spectral index through $\alpha = 2\alpha + 1$.

Esence of DM and thermal gas, Coma cluster also shows hints for the presence of relativistic particles in its atmosphere. The main evidence for the presence of a non-thermal population of relativistic electrons comes from the observation of the diffuse radio emission at frequencies $v_r \sim 30MHz - 5$ GHz [29]. The diffuse emissions are referred to as radio halos and radio mini-halos when they appear projected on the center of the cluster, while they are called relics when they are

found in the cluster periphery. Additional evidence for the presence of non-thermal phenomena in clusters of galaxies comes from the detection in a number of cases of EUV excess emission and of HXR excess emission.

The nature and properties of large-scale radio halos and relics are poorly known, because of observational and theoretical difficulties in studying these plasmas on large scales (e.g. spectral steepening as a function of distance from the center of the cluster is one of the most challenging peces of information to be explained [30]. Due to synchrotron and inverse Compton losses, the typical lifetime of the relativistic electrons in the ICM is relatively short ($10^8 yr$), making it difficult for the electrons to diffuse over a Mpc-scale region within their radiative lifetime [31]. i.e. If electrons are accelerated in discrete sources in the central regions of clusters, the severe energy losses and the diffusive motion force the electrons to cover at most distances of order of a few kpc from the source, while diffuse radio emission is clearly observed on Mpc scales [32]. To solve this problem, re-acceleration models have been invoked which describe the mechanism of energy transfer into the relativistic electron population as well as the origin of relativistic electrons. Current proposed models for radio halos can be grouped in two main classes, involving primary electrons and secondary electrons [31].

2.2.1 Primary electrons

In the primary electrons model of the origin of relativistic electrons, relativistic particles such as cosmic ray electrons and protons are believed to be injected in galaxy clusters volume by the energetic sources during the cluster dynamical history. These energetic sources are mainly due to AGN activity and star formation in normal galaxies (galactic winds and supernovae) [31]. Thus according to this model electrons can be accelerated in shocks by the mechanism of Diffusive Shock Acceleration (DSA) [33]. This mechanism has been invoked several times as the main acceleration process in clusters of galaxies that have been involved in a merger event [34].

However, it has been suggested that these populations of electrons needs to be re-accelerated in order to compensate for their radiative losses [35]. In the primary electrons model electrons have short lifetime as compared to the age of the cluster and, as a result of the energy losses, they travel short distance as compared to the size of a radio halo this is the problem of this model. The approximate distance the electron travel will be ~ 50 kpc which is far less in comparison with typical scale of a radio halo $(\sim)$ Mpc. Because of this the electrons will be confined to the

region where they were initially accelerated and they will be limited to produce synchrotron emission for a short period of time. This phenomena, however, contradicts with the observed extended diffuse synchrotron emission at a larger scale as well as the relative abundance of the electrons.

2.3 Models for the origin and evolution of particles giving rise to diffuse sources

Since magnetic fields are found to be ubiquitous in galaxy clusters a very crucial ingredient for the existence of diffuse synchrotron radio sources is the presence of relativistic particles. Radio halos are most difficult to explain, because of their very large size. Radiating electrons cannot travel such large distances within their lifetime, because of strong radiative losses by synchrotron and inverse Compton emission. Three main classes of models have been suggested for the origin of relativistic electrons present in the cluster volume and responsible for the diffuse radio emission: the primary electron model which predict that relativistic particles are continuously accelerated in the cluster volume, the secondary electrons model in which relativistic electrons are produced throughout the cluster by pp collisions and a model that suggests DM annihilation processes as a source of relativistic electrons [27].

2.4 Non-thermal emission from galaxy clusters

Beyond the presence of DM and thermal gas, Coma cluster also shows hints for the presence of relativistic particles in its atmosphere. The main evidence for the presence of a non-thermal population of relativistic electrons comes from the observation of the diffuse radio emission at frequencies $v_r \sim 30MHz - 5$ GHz [29]. The diffuse emissions are referred to as radio halos and radio mini-halos when they appear projected on the center of the cluster, while they are called relics when they are found in the cluster periphery. Additional evidence for the presence of non-thermal phenomena in clusters of galaxies comes from the detection in a number of cases of EUV excess emission and of HXR excess emission [36].

The nature and properties of large-scale radio halos and relics are poorly known, because of observational and theoretical difficulties in studying these plasmas on large scales (e.g. spectral steepening as a function of distance from the center of the cluster is one of the most challenging peces of information to be explained

[30]. Due to synchrotron and inverse Compton losses, the typical lifetime of the relativistic electrons in the ICM is relatively short ($10^8 yr$), making it difficult for the electrons to diffuse over a Mpc-scale region within their radiative lifetime [31]. i.e. If electrons are accelerated in discrete sources in the central regions of clusters, the severe energy losses and the diffusive motion force the electrons to cover at most distances of order of a few kpc from the source, while diffuse radio emission is clearly observed on Mpc scales [32]. To solve this problem, re-acceleration models have been invoked which describe the mechanism of energy transfer into the relativi-stic electron population as well as the origin of relativistic electrons. Current proposed models for radio halos can be grouped in two main classes, involving primary electrons and secondary electrons [31].

2.4.1 Re-accelerated Electrons

Re-accelerated electrons model is a sub-category of the primary electrons model. Cosmic ray electrons that are injected by different processes listed above are expect-ed to be accelerated again (re-energized) by turbulence processes which produce waves, possibly associated with the merger history of the cluster. Moreover, at each re-acceleration step, the total energy in accelerated particles can be substant-ially increased if the shocks are sufficiently strong. i.e. the merger is small (mergers between clusters with very different masses). Low energy electrons, which may also be confined for a few billion years with no appreciable energy loss within the clusters, may also be re-energized by the passage of merger shocks, so that for the duration of the merger they can reach the relativistic energies required to produce the non-thermal radiation observed in the radio bands. [37]

2.4.2 The secondary electron model

In the hadronic model, secondary electrons are injected as secondary particles by inelastic nuclear collisions between the relativistic protons and the nuclei of the thermal ambient intra cluster medium. The protons diffuse on large scale because their energy losses are negligible. They can continuously produce in situ electrons, distributed through the cluster volume. The reactions that lead to the production of secondary electrons are described by the secondary electron model:

$p + p \rightarrow \Pi^{\pm} + X$ where X represents any reachable final state from the initial state. The charged pions ($\Pi^{\pm}$) will decay into electrons, positrons and neutrinos via

muons; $\Pi^+ \rightarrow \mu^+ + \nu_\mu$

$\Pi^- \rightarrow \mu^- + \bar{\nu}_\mu$ and $\mu^+ \rightarrow e^+ + \nu_e + \bar{\nu}_\mu$

$\mu^- \rightarrow e^- + \bar{\nu}_e + \mu$

Similarly, the neutral pions (Π^0) will decay predominantly into γ-rays:

$P + P \rightarrow \Pi^o + X$,

$\Pi^0 \rightarrow \gamma + \gamma$

Secondary electron models can reproduce the basic properties of the radio halos provided that the strength of the magnetic field averaged over the emitting volume is larger than a few μG. In this case, they predict synchrotron power-law spectra, which are independent of cluster location, i.e. do not show any features and/or radial steepening, and the spectral index values are flatter than $\alpha \sim 1.5$. Some of the problems of the secondary model include, the steepening at high frequencies of the Coma radio halo spectrum, the change of the spectral index along the cluster, and the worst problem being the lack of gamma ray detection [36].

2.4.3 Dark matter annihilation/decay processes

The third model suggested as a possible source of relativistic secondary electrons and positrons is from DM annihilation/decay processes in the galaxy clusters. In this model DM annihilation/decay processes are believed to produce a wide range of SM particles and radiations such as electrons, positrons and gamma-ray radiations. Electrons and positrons will undergo energy losses while interacting with particles in ICM and will emit in a multi wavelength spectrum after reaching equilibrium states through various emission mechanisms (see section 3.3). A number of DM particle candidates have been proposed in the light of particle physics models, which are expected to produce indirect signals through annihilation/decay processes. WIMPs are the largest class of cold DM candidates among which neutralinos are the most stable particles that arise in extensions of the SM particle physics, see [34] for more. Neutralinos are called Majorana type of particles, thus they are their own anti-particles. Through their self-annihilation they produce unstable SM particles such as neutral and charged pions. This neutral and charged pion will then decay into radiation (gamma rays) and particles (relativistic $e^\pm$), respectively. When these secondary $e^\pm$ interact with the magnetic field and charged particles in the intra-cluster medium (ICM) they produce radio signals through synchrotron emission processes, and gamma rays from bremsstrahlung and Inverse Compton

Scattering (ICS) processes [17] .

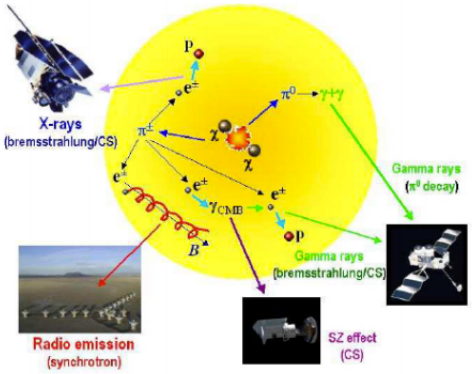

Figure 2.3: Graphical representation of multi-wavelength emission from neutralino annihilation process

[17]

Several authors have studied the astrophysical results of these assumptions laid on secondary electrons from DM annihilation/decay processes . One common strength of these previous studies lies in their ability to reproduce the observed steepening in the flux spectrum, the spectral energy distribution, at higher radio frequencies of the Coma cluster. This can be understood to be due to the fact that the spectrum of secondary electrons steepens when the energy of the electrons is comparable to the mass of neutralinos. [38]

2.5 The Dark Matter model

A 9 or 60 GeV neutralino supersymmetric particle is expected to annihilate in quarks and leptons. Direct annihilation into light fermions is helicity suppressed, so that the main remaining channels of annihilations are $b\bar{b}$ and $\tau^+\tau^-$. Electrons and positrons will be, then, mainly produced through secondary processes of hadronization and/or decay. Direct annihilation into γ rays happens at 1-loop level and is therefore highly suppressed too. The bulk of photons arises from the $Pi^0 \rightarrow \gamma$ e.m. decay. In addition to the a forementioned channels, a 500 GeV supersymmetric particle can also annihilate into gauge bosons, heavy quarks and Higgs particles. The yield of photons produced in these cases, as well as their energy spectrum, is very much similar to each other, so that we choose as a representative case the annihilation into WW^- [39].

2.6 Short and brief summary of the chapter

This chapter is mainly concerned with the observed radio emission from clusters which is not related to the individual galaxies of the clusters. However, at present the origins of neutralino emission in galaxy clusters is not well understood. The source of this relativistic electrons which are responsible for the radio emission were suggested by different models. According to the primary model the transfer of energy from the cluster ICM to the radiating particles is due to the cluster turbulence and cluster shocks. In the hadronic model the secondary electrons are injected as secondary particles by inelastic nuclear collisions between the relativistic protons and the nuclei of the thermal ambient intra cluster medium. According to the third model, which is the interest of this work, the source of the relativistic electrons is the DM annihilation processes in the galaxy clusters.

CHAPTER 3

Data presentation and analysis

3.1 Introduction

To explore diffused radio emission from galaxy clusters we have considered DM annihilation or decay processes as a source of relativistic electrons. We have applied this model on a sample of simulated Coma like galaxy clusters obtained from cosmological simulations. Cosmological simulations are a powerful and important tool in order to understand the cosmos.

A detailed simulation can provide an important information about the processes which occur on such long time scales (millions or billions of years) in which impossible to observe these events in the Universe. Cosmological simulations are also used to study galaxy collisions and also the formation of large scale structure in the Universe [40]. In the following paragraphs we have introduced different cosmological simulation datasets available from which we have selected one for the sake of our research.

There are many cosmological methodes. Among them the GADGET, which is a simulation code for galaxy collisions or for early structure formation in the Universe computes gravitational forces with a hierarchical tree algorithm (optionally in combination with a particle-mesh scheme for long-range gravitational forces) and represents fluids by means of smoothed particle hydrodynamics (SPH) [41]. The code can be used for studies of isolated systems, or for simulations that include the cosmological expansion of space, both with or without periodic boundary conditions. The most accurate cosmological simulation to date of the evolution of the largescale structure of the Universe is the Bolshoi simulation [42].

The principal purpose of the Bolshoi simulation is to compute and model the evolution of DM halos, thereby rendering the invisible for astronomers to study, and to predict visible structure that astronomers seek to observe [43]. Bolshoi has given cosmologists a fairly accurate picture of how the Universe actually evolved. It is currently being analyzed in preparation for publication and distribution of its

results in 2014. For further information visit: BolshoiCosmologicalSimulation-Wikipedia.html. MUltidark SImulation of galaxy Clusters (MUSIC)-dataset is a large subset of a mass limited sample of resimulated clusters selected from the MultiDark Simulation which is a DM only N-body simulation with 2048 particles in a $1h^{-1}Gpc$ cubic box.
This simulation run was done using the best-fit cosmological parameters to $WMAP7$ + BAO + $SNI(\Omega_m = 0.27, \Omega_b = 0.0469, \Omega = 0.73, \sigma_8 = 0.82, n = 0.95, h = 0.7)(Jarosiketal., 2011)$.
The MUSIC clusters have a large numbers of samples (282 clusters and thousands of groups) and a high resolution[44].

3.2 Data presentation

To determine the DM annihilation flux from neutralino χ in galaxy clusters, we have used the MUSIC-dataset as our first data source. The data in the MUSIC simulation contain the particle mass and coordinates divided into different mesh or grids (i.e, 21, 101, 201, 401, or 801).
From this large number of samples avialable on the MUSIC-dataset we have taken a simulated Coma like galaxy cluster namely, SGC280 where the sample selection was done to optimize the resolution and computation time. Therefore, our sample SGC280 is divided by 201 grids allowing us to obtain comparatively good resolution and low computation time.
The second data source that we have taken into account is the DarkSUSY package, a fortran package that calculate the yield of different particles per a neutralino annihilation.
In this package the simulation is done for 8 fundamental annihilation channels $c\bar{c}$, $b\bar{b}$, $t\bar{t}$, $\tau^+\tau^-$,W^+W^- , Z^OZ^O, $g\bar{g}$ and$\mu^+\mu^-$ and different masses of neutralino [45].
For our specific case we have taken the production (initial) spectra of electrons per neutralino annihilation for a neutralino mass of 9 GeV , 60 Gev dominated by $b\bar{b}$ and $\tau^+\tau^-$ species and also 500 GeV with W^+W^- and $\tau^+\tau^-$ species.

3.3 Dark matter annihilation model

To constrain dark matter parameters, we assume that all of the radio flux observed originates from the synchrotron radiation of the electron and positron pairs produced by dark matter annihilation [46].
Since the radio synchrotron emission is expected as a natural by-product of the self annihilation of super-symmetric DM particle, we have studied the synchrotron

emission in galaxy clusters by considering the annihilation of neutralino which is mainly composed of $b\bar{b}$,$\tau^+\tau^-$andW^+W^- species. For the annihilation channels we have considered a branching ratio of 1 In the following subsections we present the necessary mathematical expressions that will help us to model the sychrotron emission from the annihilation process of WIMPs.

3.3.1 DM distribution

While discussing indirect detection mechanism of DM, it was stated that the DM particle annihilation rate is proportional to the square of DM density. Therefore, it is crucial to begin by specifing how we model the DM density taking the DM information (masses of the DM particles and their positions) from the MUSIC-dataset. And then we used the smooth-particle-hydrodynamics (SPH) kernel to determine the DM densities on a grid (see section 3.4). In Fig. 3.1 we have shown the square of DM density maps for SGC280, which is produced for our galaxy clusters according to the dataset avialable on the MUSIC database.
The brightest colors in the map clearly show enhanced DM density structures which are required to correctly determine emissions from DM annihilation processes in the cluster.

3.3.2 Magnetic Field and Thermal Plasma Models

In order to treat the diffusion of WIMP annihilation products, as well as resulting synchrotron radiation, we must account for the presence of both magnetic fields and a thermal plasma within host halos. For the thermal plasma density we assume it follows a radial scaling of the form

$$n(r) = n_o((1 + \frac{r}{r_s})^2)^{-q_e} \tag{3.1}$$

with the central value n_o and the scaling exponent q_e being specified as parameters. Then $\bar{n}$ is simply the volume average of $n(r)$ assuming spherical symmetry.

In order to determine the DM annihilation signals from the synchrotron emission we also need to model the magnetic field. In [28] two magnetic field models were used for this purpose, these are magnetic field Model A and Model B presented below: (i) Model A is a model that evaluate the magnetic field strength from the gas distribution. The magnetic field profile in this case is given by

$$B(r) = B_o(1 + (\frac{r}{r_s})^2)^{-q_b} \tag{3.2}$$

where B_o is the central magnetic field strength of the Coma cluster r is the radial distance from the cluster center r_s, is the scale radius of the DM density profile and q_b is scaling exponent choosen to be 0.5 [47]. (ii) Model B is a magnetic field model which uses the best observational value for a central magnetic field in the Coma Cluster equal to $4.7\mu G$ (at electron number density of $3.44 \times 10^{-3} cm^{-3}$) from [48]. The magnetic field B of the galaxy cluster is related to the electron number density n_e by B = $4.7\mu G(\frac{n_e}{\Pi} \times 10^{-3} cm^{-3})^{0.5}$

The electron number densityn_e in cm^{-3} is evaluated as in [44], n_e =$N_e \rho_{gas}(1ZY_{He})/m_p$, where$N_e$,ρ_{gas} , Z,Y_{He} = 0.25 and m_p are the number of ionized electrons per hydrogen atoms, gas density, metallicity, helium concentration and proton mass, respectively. We have considered magnetic field Model A following the conclusion from [28] and determined the magnetic field strength in each cube of size 10 kpc.

The magnetic field profiles for these two magnetic field models discussed above are shown in Figure. 3.2.

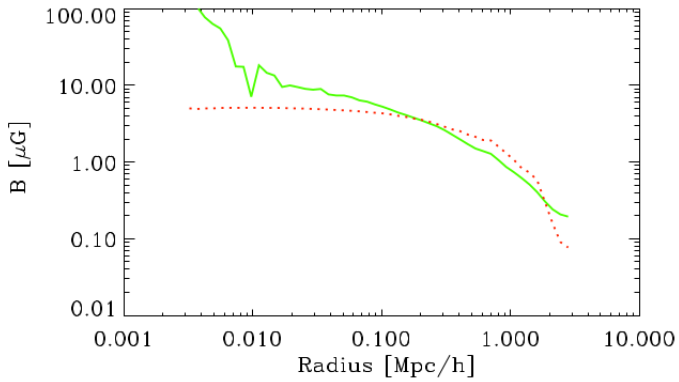

Figure 3.1: Magnetic field profiles of the two magnetic field models: Model A and Model B are shown in red dotted line and green solid line, respectively [28].

3.3.3 Electron Source Functions From Neutralino Annihilations

In this paper we assume dark matter to be composed of the lightest neutralino from the minimal supersymmetric extension to the standard model, following the model used by the DarkSUSY package [45] . The source function for the production of a stable particle i, produced promptly by neutralino annihilation processes is given

by

$$Qi(r,E) =< \sigma\nu > \Sigma_f(\frac{dN_i^f}{dE}B_f N_x(r)) \tag{3.3}$$

where$< \sigma\nu >$i is the thermally-averaged neutralino annihilation cross-section at 0 K, the index f labels .kinematically justified annihilation final states with branching ratios B_f and spectra $\frac{dN_i^f}{dE}$, and $N_\chi(r)$ is the neutralino pair density at a given halo radius r. the chosen particle physics framework will dictate both $< \sigma v >$ and the set of branching ratios.

Since the neutralino is a Majorana fermion, light fermion final states are suppressed in favour heavy fermions and Higgs bosons. In keeping with standard procedure in indirect detection studies we will focus on one annihilation channel at a time and assume a branching ratio of 1 for the channel of interest.

In this study we have focussed on the $b\bar{b}$,W^+W^- and $\tau^+\tau^-$ annihilation channels, and employed the python code in order to determine the $\frac{dN_i^f}{dE}$,for electron production from the decay of neutralino annihilation products. Finally, the neutralino pair density will be calculated in accordance with equqtion 3.2

$$N_x(r) = \frac{((\rho_{tot} - f_s M_{vir} p_{sub}(r))^2 + p_{sub}(r)B)}{2M_x^2} \tag{3.4}$$

$N_x(r)$ can then be expressed as $\frac{\rho_{DM}^2}{2M_x^2}$, where the factor 2 in the denominator appears to take into account the annihilating pairs [47].

3.3.4 The equilibrum spectra of emitting particles

The electrons equilibrium spectra are obtained from the "source spectra" of the injected electrons by considering their energy loss by different mechanisms, and their spatial diffusion process as they pass through the atmosphere of the DM halo [20]. This process is governed by the diffusion equation in the following form:

$$\frac{\partial}{\partial t}\frac{dn_e}{dE} = \bigtriangledown(D(E,X) \bigtriangledown \frac{dn_e}{dE}) + \frac{\partial}{dE}(b(E,X)\frac{dn_e}{dE})), \tag{3.5}$$

where $\frac{dn_e}{dE}$ is the $e^\pm$ equilibrium spectrum, D(E, x) is the spatial diffusion function, b(E, x) is the energy-loss function and $Q_e(E,x)$ is the electron source function. A detailed analysis of the solution to this equation in the case of electron production via neutralino annihilation can be found in [29].

A generic solution to the diffusion equation which in the case of galaxy clusters, where the effect of diffusions of electrons are negligible, is given by[29]. This solution which is the "electrons equilibrium spectra" has the form:

$$\frac{dn_e}{dE}(r,E) = \frac{1}{b(E)} \int_E^{M_x} dE\prime G(r,E,\prime) Q_e(r,E\prime), \tag{3.6}$$

where E is the energy of the electrons and b(E) (see Eq. 3.7)is the energy loss term in units of$GeVs^{-1}$ which is the sum of effects due to ICS, synchrotron radiation, $G(r,E,E\prime)$ is a Green's function which will reduce to unity in the case of larger halos at zero Coulomb losses and bremsstrahlung radiation [29].

$$b(E) = b_{IC}E^2(1+z)^4 + b_{sync}E^2\bar{B}^2 + b_{coun\bar{}}(1+z)^3(1+\frac{1}{75}log(\frac{\gamma}{\Pi(1+z)^3}))+b_{brem}\bar{n}(1+z)^3(log(\frac{\gamma}{\Pi(1+z)^3})+0.36)$$

(3.7)

Where $\gamma = \frac{E}{m_e}$ and b_{IC} ,b_{synch} ,b_{coul} , and b_{bream} are the Inverse Compton Scattering, synchrotron, Coulomb and Bremsstrahlung energy loss factors in units of $GeVs^{-1}$, respectively. The "electrons equilibrium spectra" can be used to calculate the local emissivities and ultimately the flux, which will be used in the following section [29].

3.3.5 Synchrotron Emission

The average power of the synchrotron radiation at observed frequency ν emitted by an electron with energy E in a magnetic field with amplitude B is given by[49]:

$$P_{synch}(v,E,r,z) = \int_0^{\Pi} d\Theta \frac{sin^2\Theta}{2} 2\Pi\sqrt{3} r_e m_e c v_g F_{synch}(\frac{k}{sin\Theta}) \tag{3.8}$$

where m_e is the electron mass, ν_g = $\frac{eB}{2\Pi m_e c}$ is the non-relativistic gyro-frequency, r_e=$\frac{e^2}{m_e c^2}$ classical electron radius, and the quantities k and F_{synch} are defined as:

$$k = \frac{2\nu(1+z)}{3\nu_o\gamma^2}(1+(\frac{\gamma\nu_p}{\nu(1+z)})^2)^{3/2}, \tag{3.9}$$

$$F_{synch}(x) = x\int_x^{\infty} dy k_{5/3}(y) \cong 1.25x^{1\succ/3}e^{-x}(648+x^2)^{1/12}, \tag{3.10}$$

The local synchrotron emissivity can then be found as a function of the electron and positron equilibrium distributions as well as the synchrotron power

$$j_{synch}(v,r,z) = \int_{m_e}^{M_x} dE(\frac{dn_{e^-}}{dE} + \frac{dn_{e^+}}{dE} p_{synch}(v,E,z) \tag{3.11}$$

Once one has determined this quantity, it can be used to find all of the observables relevant to our study, namely the flux densities and surface brightnesses of the dark matter halo. The flux density spectrum within a radius r is found via

$$S_{synch}(v,z) = \int_0^r d^3r\prime \frac{j_{synch}(v,r\prime,z)}{4\Pi D_L^2}, \tag{3.12}$$

where D_L is the luminosity distance to the halo. Then the azimuthally averaged surface brightness is given by

$$I_{synch}(v,\Theta,\Delta\Omega,z) = \int_{\Delta\Omega}\int_{l.o.s} dl \frac{j_{synch}(v,l,z)}{4\Pi}, \tag{3.13}$$

where the integrals are performed over a cone given by the solid angle $\Delta\Omega$ and an axis along the line of sight (l.o.s) which makes an angle Θ with the direction of the halo centre [29].

3.4 Data analysis

The raw data we have taken from the MUSIC simulation contains the DM particle, coordinates and mass simulated galaxy clusters. From this raw data for the position and mass of DM particle, we used SPH-kernel to determine the density of DM on a grid [50].

Next to this important procedures, we used a fortran code to allocate the DM and gas density on a three dimensional cube of side 2 Mpc which is grided into smaller cubes of side $\sim$10 kpc (the simulated galaxy clusters which are $(2Mpc)^3$ in volume are divided into $\sim$8 millon small cubes of side $\sim$10 kpc making 201 grids on each side of the cluster. Thus, for one side of the clusters the grids give about 40,401 square boxes). Now knowing the DM and gas density in each cube help us to determine and allocate the magnetic field and electron density within the cluster which inturn allow us to compute the gyro- and plasma frequency,

respectively according to the relation given under subsection 3.3.5. Combining this results with the electron production spectra from the DarkSUSY package (a fortran package that calculate the yield of particles per a neutralino annihilation and our second data source) enables us to calculate all the necessary ingrediants. For the synchrotron emission i.e, the electron source factor $Q_e(E, r)$, the electronequilibrium spectra $\frac{dn_e}{dE}$ and the average power radiated $P(\nu, E, r, z)$ according to the Eqns. 3.3, 3.6 and 3.8, respectively. Finally, the local emissivity and the integrated flux density are computed in each cube based on Eqns. 3.11 and 3.12. In addition to the fortran program we have also used python to produce all our maps.

CHAPTER 4

Results and Discussion

4.1 Introduction

If WIMPs (neutralinos) are indeed the leading DM candidates, the question remains, how do we begin to detect these particles? One way is to look at products of neutralino annihilation. Neutralinos are theorized to have a mass in the range 10 GeV to Tera eV , be electrically neutral and to also be their own anti-particle. Because of this, neutralino are thought to annihilate into standard model particles like fermions or gauge bosons.

$$\chi + \chi \rightarrow f + f^{-}, W + W^{-}, Z^{0} + Z, ...[51]. \tag{4.1}$$

We can begin to look for these annihilation signatures from areas in the universe that are thought to be dominated by dark matter. One of the better solution is to scan the universe for radio emission resulting from dark matter annihilation. In this thesis there are three dark matter annihilation channels that are considered.

$$\chi\chi \rightarrow b\bar{b} \tag{4.2}$$

$$\chi\chi \rightarrow \tau^{+}\tau^{-} \tag{4.3}$$

$$\chi\chi \rightarrow W^{+}W^{-} \tag{4.4}$$

The three annihilation channels used in this analysis were chosen for several reasons. Due to the available phase space, dark matter is expected to annihilate into the heaviest available channel, thus we consider the hevey tau lepton ($\tau^{+}\tau^{-}$) channel. The $b\bar{b}$ annihilation channel is included since it has been studied by several experiments (Fermi-LAT, MAGIC, etc.) to allow for direct comparison of results. The bosonic $W^{+}W^{-}$ channel was chosen since it is the standard boson channel and also widely considered in other experiments.

The two frequencies were chosen to represent the SKA-low frequencies. The radio emission maps produced in this thesis are using constant magnetic field model. Annihilation of dark matter can result in the production of stable SM particles including electrons and positrons that, in the presence of magnetic fields, lose energy via synchrotron radiation, observable as radio emission. Galaxy clusters are excellent targets to search for or to constrain the rate of DM annihilation, as they are both massive and DM dominated.

In the following sections and subsections we will mention and describe the procedures stated in the previous chapters, which were studing the characteristics of DM particle species potentially responsible for the diffused radio emission, by DM annihilation or decay processes from the Coma like simulated galaxy cluster.
For this reason, we base our study of synchrotron or radio emission by taking neutralino to be annihilated or decayed into $b\bar{b}$, $\tau^+\tau^-$ and W^+W^- species. Thus we consider neutralino of mass M_x= 9 GeV, 60 GeV and 500 GeV taking the thermally averaged DM annihilation cross-section times velocity, $< \sigma\nu >$, to be $1.0 \times 1o^{-26} cm^{-3}$ from Fermi upper limit [52].
For the sake of studying the diffused radio emission from the Coma cluster, DM annihilation/decay processes as the sources of relativistic electrons and the mathematical models discussed in section 3.2 have been applied to compute the synchrotron emission in asimulated Coma like galaxy cluster (SGC280).
The synchrotron or radio emission results obtained from DM annihilation processes in galaxy cluster (SGC280) will be presented in the following sections. The emission maps are generated based on the data set available from MUSIC cluster [53], a high-resolution cosmological simulation containing DM, gas and stars.
The emission maps are produced by dividing a 3-D cluster of 2 Mpc across into cubes of size 10 kpc. In the first section the DM distribution and the density map for the cluster has been presented. In the second part of this chapter, the radio flux and the radio emission maps produced for diffrent masses of neutralino and diffrent annhilation chaneles and frequency are discussed.

4.2 The distribution of DM within (SGC280)

The DM density squaree map shown in Fig. 4.1 is in units of $[M_\odot kpc^{-3}]^2$. It represents the DM distributed in a three dimensional galaxy cluster projected upon to a two dimensional map by integrating all the DM density along the line-of-sight. The bright yellow regions on the maps are the densest DM regions in the galaxy

cluster. The map indicates how the DM density decreases as we go from the center to the edge of the cluster except at the substructures which are far from the center. It has been discussed in section 3.2 that the cluster sides are grided into a total of 40,401(201by201) square boxes. For the sake of detecting DM we need to know from which regions of the galaxy cluster are the higher emissions coming from. But we know that the higher emissions originate from the regions of high annihilation rate which is proportional to the square of the DM density (i.e, $\Gamma_{ann} \propto \rho^2_{DM}$). So all the densest regions on the map which are near the center and off-center are our source (or amplifiers) of higher radio emission. Therefore, the DM density square map tell us where to expect for the radio emission.

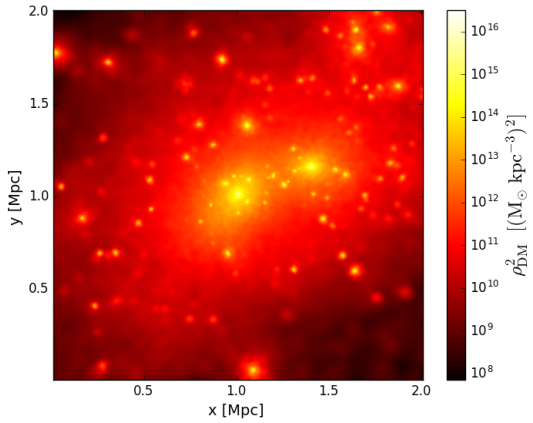

Figure 4.1: Density square map of Galaxy Cluster SGC280 obtained by using SPH kernel.

4.3 Radio flux and emission maps

At this stage, we are in position to display the results we have found for radio emissions, from diffrent DM annihilation chanels in SGC280 along with the discussion. Using the computed flux data from the simulations done so far, we are now capable to produce a good resolution maps and graphs that allow us to look for possible radio emission sources distributed in the SGC280 regions. As a result we will produce emission maps and graphs in the following subsection, for neutralino masses M_x = 9 GeV, 60 GeV and 500 GeV which annihilate into $b\bar{b}$,$\tau^+\tau^-$ and W^+W^- channels.

4.3.1 Radio flux and emission maps for M_x = 9 GeV

Figure 4.2 shows the radio emission maps obtained from DM decay process at 110 MHz frequency. These two radio emission maps were obtained from two different annihilation final state $b\bar{b}$ and $\tau^+\tau^-$ for light mass DM model M_x = 9 GeV. To know the best fit composition of DM , which is responsible for the expected radio emission from the simulated coma c like galaxy cluster.

From the emission maps of the clusters, shown in the following figure (Fig. 4.2), the bright yellow regions at the centers and substructures at off-centers are the regions of high annhilation rate as well as the regions of high DM density (the densest region of DM) since the annihilation rate is proportional to the density square as discused in the previous chapters. As a result of this, high radio emission is expected at those regions for the two channels of the cluster and they are thougt to be sources of the radio emission and dominated by DM.

When we come to compare and contrast the two channels, the dense central regions of figure $\tau^+\tau^-$ is brighter than that of figure $b\bar{b}$, indicating that the lightest mass DM model annihilates into ($\tau\tau^-$) than ($b\bar{b}$) and more radio emission is expected at $\tau\tau^-$ channel. Comparison between emission maps in figure 4.2 show no morphological difference as well as noticeable difference on the background structure of the emission. But there is a diffrence in the output flux at the two annihilation channels as can be clearly seen from the colorbar of the two maps.

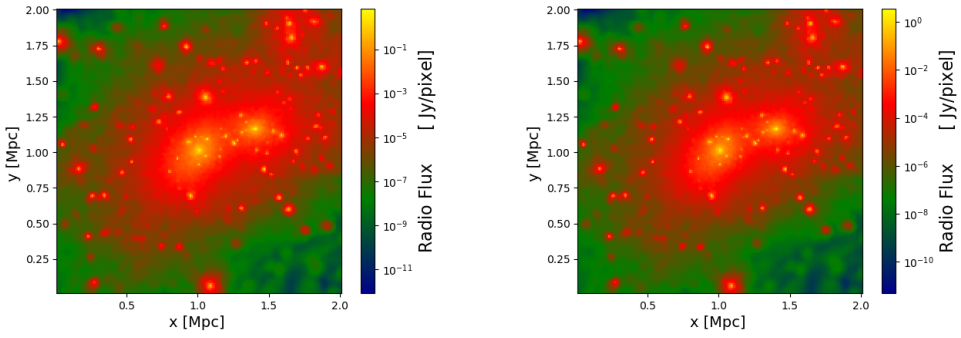

Figure 4.2: Radio emission maps from light DM mass 9 GeV annihilation into $b\bar{b}$ (left panel) and $\tau^+\tau^-$ (right panel) at 1400 MHz

Figure 4.3 shows the radio emission maps obtained from DM decay process at a frequency of 300 MHz.These two radio emission maps were obtained from two different annihilation final state $b\bar{b}$ and $\tau^+\tau^-$ for light mass DM model M_x = 9 GeV. From the emission maps of the clusters, shwon in the following figure (Fig. 4.3) the bright yellow regions at the centers and substructures at off-centers are the

regions of high annihilation rate as well as the regions of high DM density(the densest region of DM) since the annhilation rate is proportionalto the density square as discused in the previous chapters. As aresult of this, high radio emission is expected at those regions for the two clusters and they are thougt to be sources of the radio emission and dominated by DM.

When also we compare and contrast the emission maps from the two channels, the dense central regions of figure ($\tau\tau^-$) is brighter than that of figure $b\bar{b}$. Indicating that the lightest mass DM model annihilates into the lepton($\tau\tau^-$) than the bottom($b\bar{b}$) quark flavour. More over, more radio emission is expected at the lepton($\tau\tau^-$) channel. Comparison between emission maps in figure 4.3 do not show signficant morphological diffrence and noticeable difference on the background structure of the emission. But, thereis a diffrence in the output flux at the two annhilation channels as can be seen from the colorbar of the two maps.

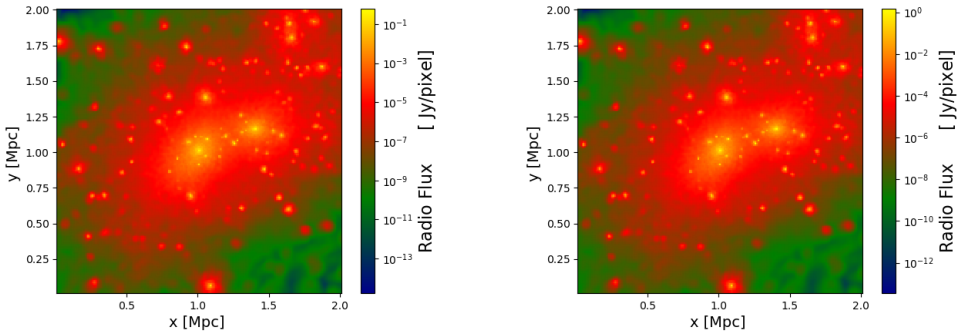

Figure 4.3: Radio emission maps from light DM of mass 9 GeV annihilation into $b\bar{b}$ (left panel) and $\tau^+\tau^-$ (right panel) at 4850 MHz

4.3.2 Radio flux and emission maps for M_x = 60 GeV

For the intermidate mass DM model M_x 60 GeV, the radio emission maps produced are presented as follows.

As indicated in Figure (4.4) there is no morphological diffrence and background structure of emissions, but there is a diffrence in output flux. The $\tau^+\tau^-$ annhilation channel produce more radio emission than the $b\bar{b}$ channel as can be seen from the two maps. Hence, the $\tau^+\tau^-$ is dominant over the $b\bar{b}$ at 1400MHz.

In figure(fig 4.5) , we have also produced emission maps for the intermidate mass DM model M_x=60 GeV, which annihilate into $b\bar{b}$ and $\tau^+\tau^-$ channels at a frequency 4850 MHz. There is no significant morphological difference observed between the

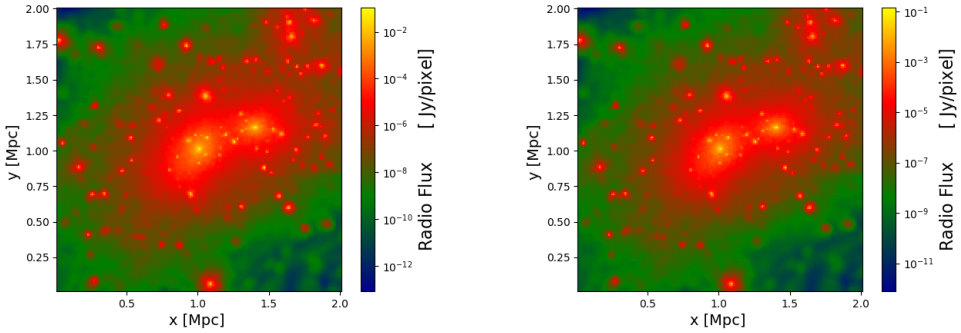

Figure 4.4: Radio emission maps from an intermidate neutralino mass 60 GeV annihilation into $b\bar{b}$ (left panel) and $\tau^+\tau^-$ (right panel) at 1400 MHz

maps at the two different annihilation channels shown in Figure 4.5. There is also no noticeable difference on the background structure of the emission but the out put flux values from the colorbars of the maps are diffrent. In addtion to this the radio emission map of $b\bar{b}$ channel is brither at the center and off center substructures than the $\tau^+\tau^-$ channel, showing more annihilation and radio emission at $b\bar{b}$.

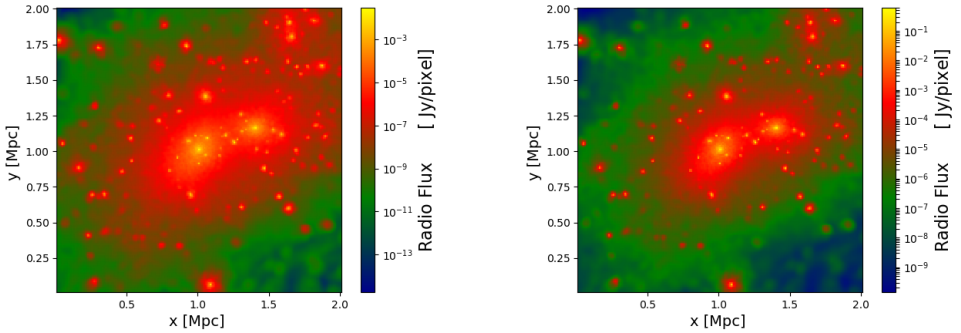

Figure 4.5: Radio emission maps for an intermediate neutralino mass used M_x=60 GeV annihilated in to $b\bar{b}$ (left panel) and $\tau^+\tau^-$ (right panel) at a frequency of 4850 MHz

4.3.3 Radio flux and emission maps for M_x = 500 GeV

In the following section, we will discuss the radio emission from the maps ploted for the high DM mass M_x= 500 GeV annihilation into $b\bar{b}$ and $\tau^+\tau^-$ channels to know its best fit compostion. As can be clearly seen from the following radio emission maps, the emission map for $b\bar{b}$ is brighter at the center and also off-center substructures . This indicates that the dark matter annihilates into $b\bar{b}$ than $\tau^+\tau^-$ channel for 110MHz. So, it is also DM dominated region of the galaxy cluster. This is to mean that more radio emission is expected from the $b\bar{b}$ channel than the $\tau^+\tau^-$.

The background structure and out put flux values for the two figures are almost similar.

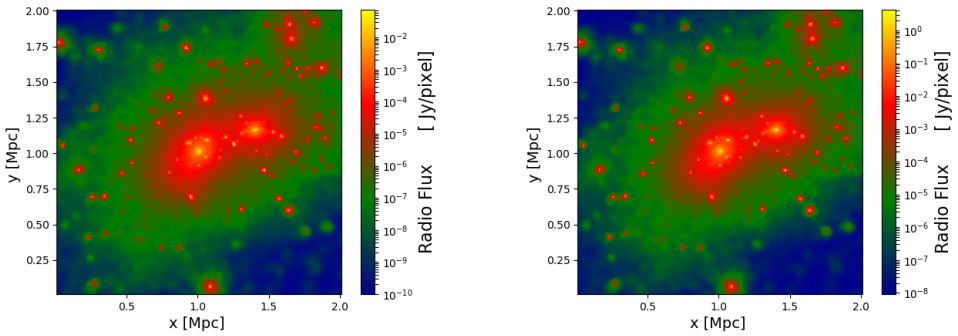

Figure 4.6: Radio emission maps for heavy neutralino mass used M_x=500 GeV annihilated in to $b\bar{b}$ (left panel) and $\tau^+\tau^-$ (right panel) at 1400 MHz

Comparison of the radio emission map for the $\tau^+\tau^-$ and W^+W^- shows the dense centeral bright and at substructures region of W^+W^- dominates over $\tau^+\tau^-$. This implies more radio emission and DM dominated region is expected at the W^+W^-.

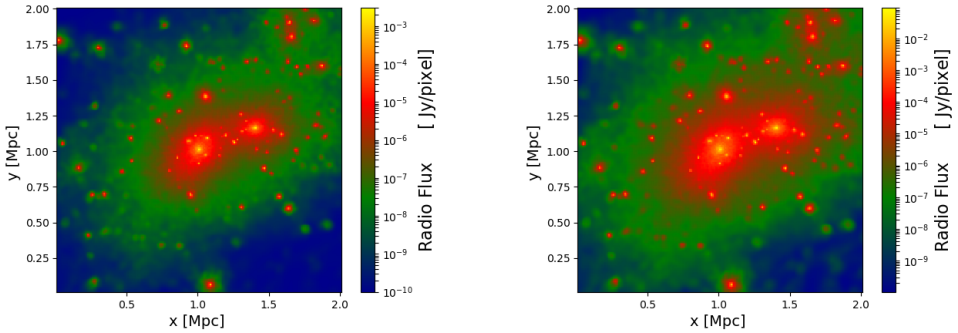

Figure 4.7: Radio emission maps for heavy neutralino mass used M_x=500 GeV annihilated in to $b\bar{b}$(left panel) and $\tau^+\tau^-$(right panel) at 4850 MHz

When we compare and contrast the two figures above, for the radio emission maps at stated channels and frequency above, we found that the the DM annhilates into the bottom-anti bottom($b\bar{b}$) quark flavour than the heavy boson-anti boson(W^+W^-). Thus more annhilation rate and more DM dominated region is expected at W^+W^- channel as discussed before. More over the difference in the output flux values indicated in the colur bars of the two maps is clearly visble.

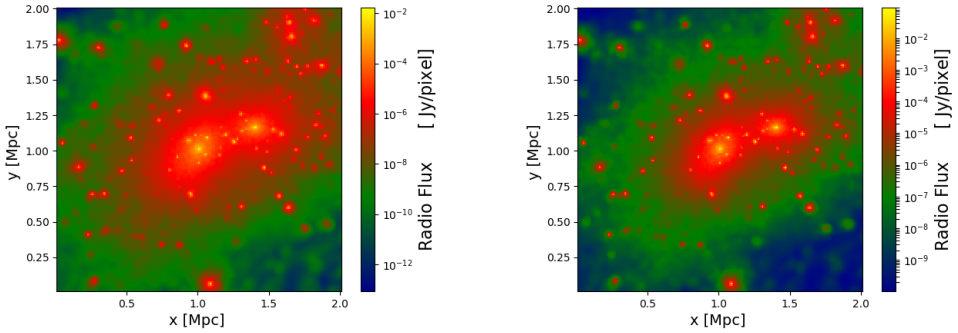

Figure 4.8: Radio emission maps for neutralino mass used M_x=500 GeV annihilation in to $b\bar{b}$(left panel) and W^-W^+(right panel) at afrequency of 4850 MHz

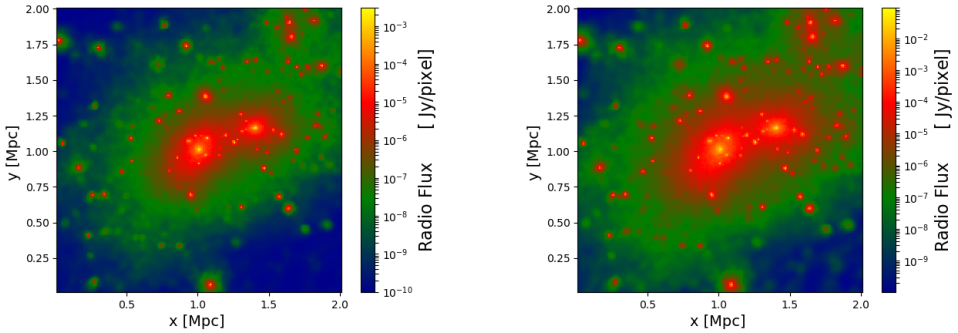

Figure 4.9: Radio emission maps for neutralino mass used M_x=500 Gev annihilation in to $\tau^+\tau^-$(left panel) and W^-W^+(right panel) at afrequency of 1400 MHz

In order to make further comparsion of the radio flux values, we have plotted the flux coming from each boxes against the radial distance of the boxes from the center of the galaxy clusters. In both cases the red colors represent flux for $\tau^+\tau^-$ and black colors represent flux for $b\bar{b}$.

The figures express the difference between the emission maps by showing that for each boxes the radio flux of both channels for $\tau^+\tau^-$ are all lower than the radio flux $b\bar{b}$. And for this reason the red color is seen shifted up. The similarity in the pattern of the profiles and the maps imply the fact that strong radio emissions at any frequency originate from the densest regions of the galaxy clusters with different flux magnitudes.

We have also plotted the flux coming from each boxes against the radial distance of

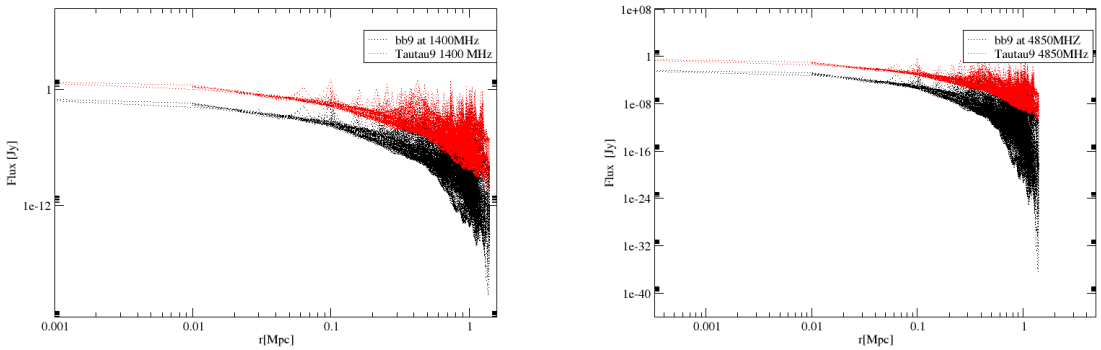

Figure 4.10: The radial distribution of the flux contribution from each boxes for DM mass 9 Gev and annihilation channels $b\bar{b}$ and $\tau^{-}\tau^{+}$ represented in black and red colors, at a frequency 1400 MHz (left panel) and a frequency 4850 MHz (right panel) respectively.

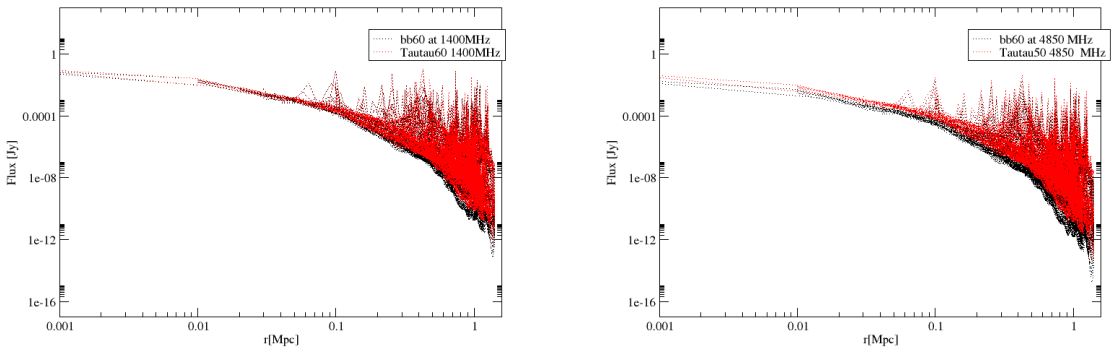

Figure 4.11: The radial distribution of the flux contribution from each boxes for DM mass 60 Gev and annihilation channels $b\bar{b}$ and $\tau^{-}\tau^{+}$ represented in black and red colors, at a frequency 1400 MHz (left panel) and a frequency 4850 MHz (right panel) respectively

the boxes from the center of the galaxy clusters as shown in Fig. 4.16 for DM mass M_x=60 Gev. In both cases the green colors represent flux for $\tau^{+}\tau^{-}$ and blue colors represent flux for $b\bar{b}$. This figures express the difference between the emission maps by showing that for each boxes the radio flux of both channels for $b\bar{b}$ are all higher than the radio flux for $\tau^{+}\tau^{-}$. And for this reason the blue color is seen shifted up. The similarity in the pattern of the profiles and the maps imply the fact that strong radio emissions at any frequency originate from the densest regions of the galaxy clusters with different flux magnitudes. In both cases the red colors represent flux for $\tau^{+}\tau^{-}$ and black colors represent flux for $b\bar{b}$. This figures express the difference between the emission maps by showing that for each boxes the radio flux of both channels for $b\bar{b}$ are all higher than the radio flux for $\tau^{+}\tau^{-}$. And for this reason the

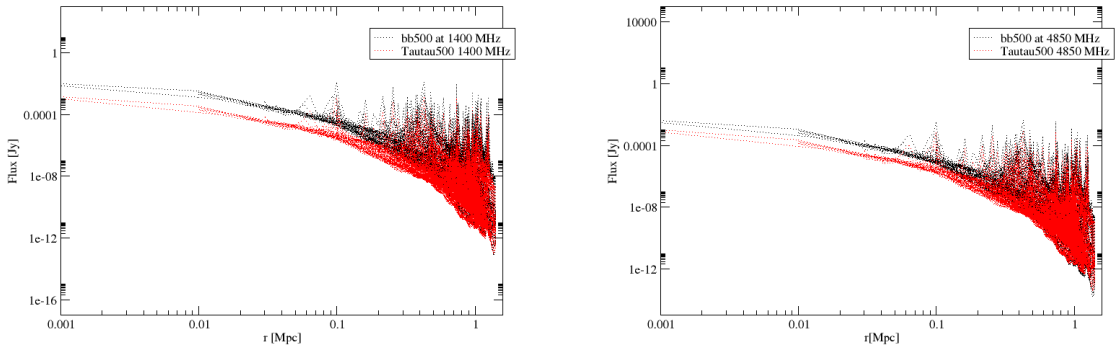

Figure 4.12: The radial distribution of the flux contribution from each boxes for DM mass 500 Gev and annihilation channels $b\bar{b}$ and $\tau^{-}\tau^{+}$ represented in black and red colors, at a frequency 1400 MHz (left panel) and a frequency 4850 MHz (right panel) respectively

blackcolor is seen shifted up. The similarity in the pattern of the profiles and the maps imply the fact that strong radio emissions at any frequency originate from the densest regions of the galaxy clusters with different flux magnitudes.
Finaly the graph of radial distribution of the flux contribution from each boxes for DM mass 500 Gev and annihilation channel $W^{+}W^{-}$, $\tau^{-}\tau^{+}$ $b\bar{b}$ is given as follows.

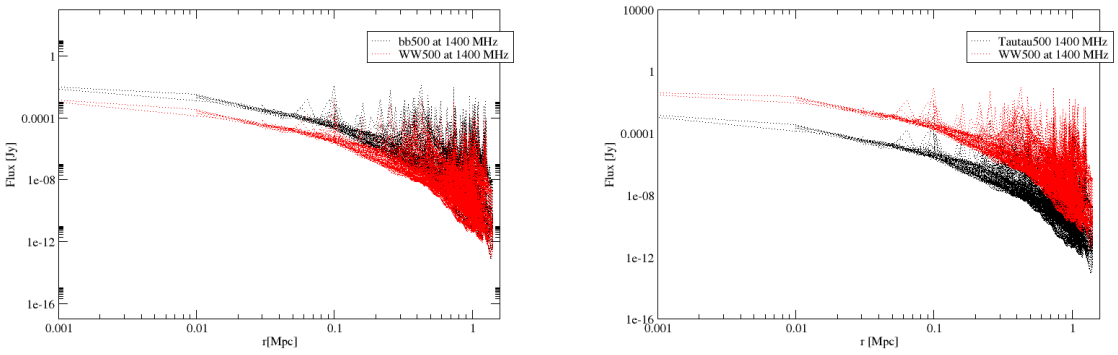

!

Figure 4.13: The radial distribution of the flux contribution from each boxes for DM mass 500 GeV, $b\bar{b}$, $\tau^{+}\tau^{-}$, $\tau^{+}\tau^{-}$ and$W^{-}W^{+}$ (left) and (right) at 1400 MHz respectively.

In the following tables(4.1, 4.2 and 4.3) we provide comparison of minimum and maximum flux values taking two annihilation channels and seven diffrent frequencies,with their corresponding integrated flux densities.

	$b\bar{b}$9			$\tau^-\tau^+$9		
Freq. [MHz]	Min.flux [Jy]	Max.flux [Jy]	Integrated flux density[Jy]	Min.flux [Jy]	Max.flux [Jy]	Integrated flux density[Jy]
30	4×10^{-11}	33	92.5	3×10^{-10}	28	481
110	8×10^{-13}	7	19	1.4×10^{-11}	11	186
300	5×10^{-15}	2	5	1×10^{-13}	5	75
608.5	2×10^{-17}	0.7	1.7	-6×10^{-14}	2.2	35
1400	5×10^{-22}	0.2	0.38	-2.2×10^{-12}	0.8	12
4850	2×10^{-37}	0.01	0.2	-3×10^{-10}	0.1	1.1
6000	2×10^{-42}	0.004	0.1	-8×10^{-10}	0.1	0.6

Table 4.1 Comparison of maximum and minimum flux values with their integrated flux for seven diffrent frequencies, $b\bar{b}$ and $\tau^-\tau^+$ annihilation channels and DM with mass M_x=9 GeV

	$b\bar{b}$60			$\tau^-\tau^+60$		
Freq. MHz	Min.flux [Jy]	Max.flux [Jy]	Integrated flux density[Jy]	Min.flux [Jy]	Max.flux [Jy]	Integrated flux density[Jy]
30	4×10^{-11}	4.4	76	4.4×10^{-11}	0.6	11
110	6×10^{-12}	2	15.6	2×10^{-11}	0.4	7
300	1.5×10^{-12}	0.6	4.1	6×10^{-12}	0.3	4
608.5	5×10^{-13}	0.3	1.4	3×10^{-12}	0.2	3
1400	8×10^{-14}	0.1	0.32	8×10^{-13}	0.2	2
4850	2×10^{-15}	0.03	0.017	5×10^{-14}	0.1	0.7
6000	7×10^{-16}	0.02	0.015	3×10^{-14}	0.1	0.6

Table 4.2 Comparison of maximum and minimum flux values with their integrated flux for seven diffrent frequencies, $b\bar{b}$ and $\tau^-\tau^+$ annihilation channels and DM with mass M_x=60 GeV

	b$\bar{b}$500			$\tau^-\tau^+500$		
Freq. [MHz]	Min.flux [Jy]	Max.flux [Jy]	Integrated flux density[Jy]	Min.flux [Jy]	Max.flux [Jy]	Integratead flux density[Jy]
30	5×10^{-12}	0.2	3	7×10^{-13}	0.003	0.06
110	2×10^{-12}	0.1	1.3	4×10^{-13}	0.004	0.05
300	5×10^{-13}	0.04	0.7	3×10^{-13}	0.004	0.04
608.5	2×10^{-13}	0.03	0.4	2×10^{-13}	0.003	0.03
1400	8×10^{-14}	0.02	0.2	10×10^{-14}	0.003	0.02
4850	2×10^{-14}	0.01	0.07	4×10^{-14}	0.002	0.02
6000	1.2×10^{-14}	0.01	0.06	3×10^{-14}	0.002	0.02

Table 4.2 Comparison of maximum and minimum flux values with their integrated flux for seven diffrent frequencies, $b\bar{b}$ and $\tau^-\tau^+$ annihilation channels and DM with mass M_x=500 Gev

4.4 Integrated radio spectrum from diffrent DM annihilation channels

By taking the sum of all the radio flux values at a given frequencey we come up with the flux density. The figures are the graph of the flux density verseus frequency, shown by the curves in blue,red,turqouise, violet, brown colors from our results of $b\bar{b}$ 9 Gev, $\tau^+\tau^-$ 9 Gev, $b\bar{b}$ 60 Gev, $\tau^+\tau^-$ 60 Gev, $b\bar{b}$ 500 Gev, $\tau^+\tau^-$ 500 Gev respectively. In the figure the observetional results from [54] for the diffuse radio halo source coma clusters are shown in blue dots for the purpose of comparision. From the curves we can see that the flux density decreases as frequency increases in all cases. This is because of the fact that particles with high energey have short radative life time than the lower energetic ones and the emission spectrum is modified accordingly due to the deplation of the high energy particles from the energy distrbution [54]. Our flux density results for $b\bar{b}$ 9 GeV is in a good agreement with the observational result of [54]. In general, in this chapter we have presented the results from the DM annihilation of neutralino for the simulated coma like galaxy clusters using the raw data taken from the MUSIC-datd set. The results enable us to produce a good resolution radio emission maps that allow us to look for possible structures and substructurs in cluster region which are required to obtain the expected radio emission from DM annihilation process. The radio emission maps and the square of DM density maps were found to be identical proving the fact that higer emission originate from the densest structures. The integrated radio spectrum declines as

frequencey increases because of the radative life time of the relativstic electrons. The flux density curve has shown that the radio spectrum of the $b\bar{b}$ 9 GeV discused above is in a good agreement with the observed radio spectrum of coma c cluster of galaxies.

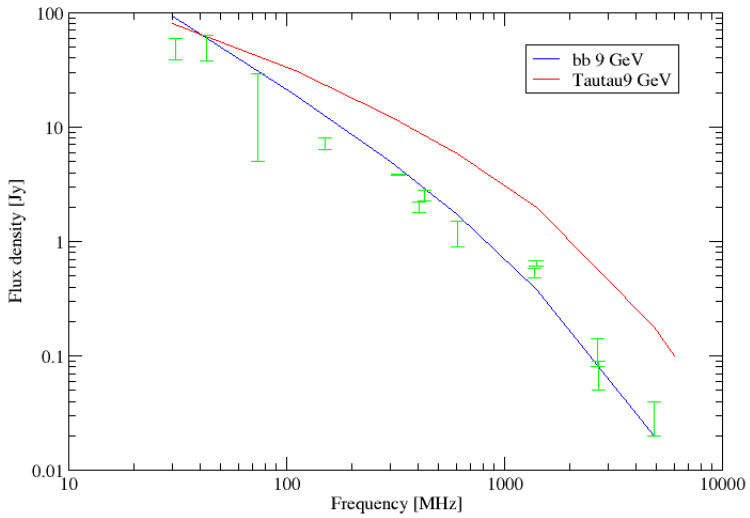

Figure 4.14: Flux density from synchrotron emission of $b\bar{b}$ 9 GeV and $\tau^{-}\tau^{+}$ 9 GeV in blue and red curves respectively in comparision to the observetional data of radio emission of coma cluster from [54] indicated in green dots

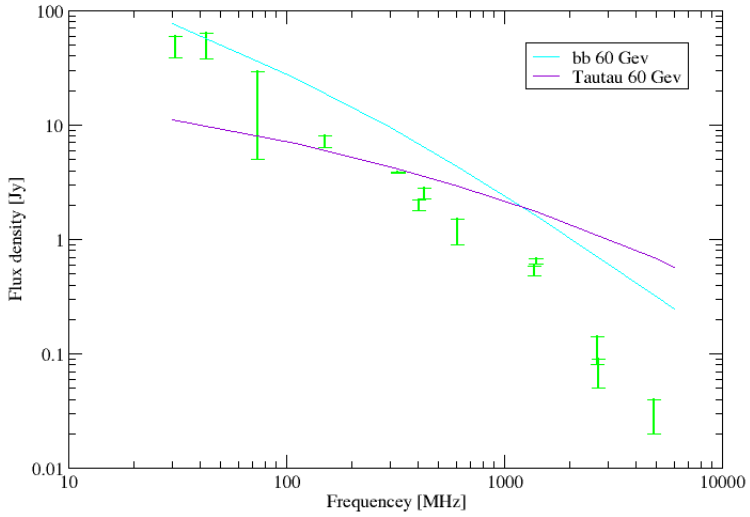

Figure 4.15: Flux density from synchrotron emission of $b\bar{b}$ 60 GeV and $\tau^{-}\tau^{+}$ 60 GeV in turqouise and violet curves respectively in comparision to the observetional data of radio emission of coma cluster from [54] indicated in green dots

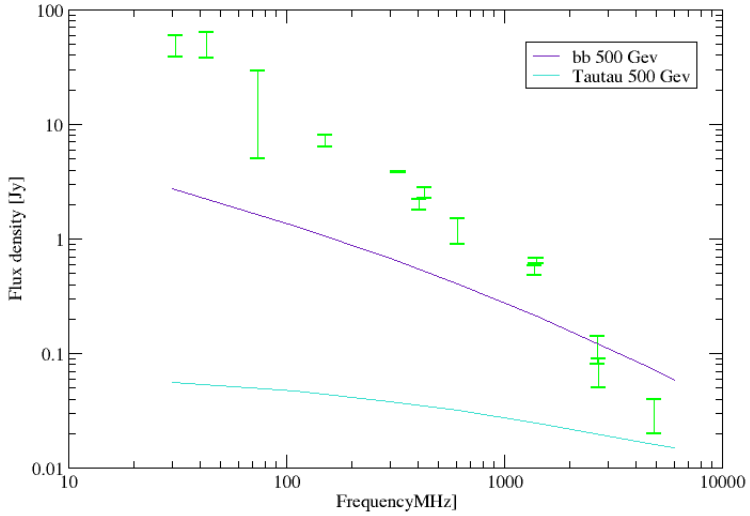

Figure 4.16: Flux density from synchrotron emission of $b\bar{b}$ 500 GeV and $\tau^{-}\tau^{+}$ 500 GeV in violet and cyan curves respectively in comparision to the observetional data of radio emission of coma cluster from [54] indicated in green dots

CHAPTER 5
Discussion and conclusions

DM is the dominant component of galaxies and clusters of galaxies. It plays a great role in the formation and morphological evolution of these huge gravitationally bounded systems, nevertheless its true nature is still elusive. As a result of this, several detection techniques have been used so far and large number of indirect investigations suggest that, the bulk matter content of the universe is invisible or dark. Thus, we have investigated DM indirectly by studying the non-thermal radio emission from their annihilation scenario in simulated Coma like galaxy cluster.

We have computed the intensity of the radio signal which depends on factors like the value of the annihilation cross section, the magnetic field intensity and density of DM particles, considering a neutralino mass of M_x = 9 GeV, 60 GeV, 500 GeV in a simulated Coma like galaxy cluster, whose raw data for the particles mass and coordinate are taken from the MUSIC-dataset. In addtion to this, we determined the density of the DM particle which is a useful tool to find out the distribution of DM in galaxy cluster by applying SPH kernel.

Radio emission maps give information about the source of radio emission, which comes from the more denser region and decreases far from the center of the cluster. And also all the radio emission maps are morphologically similar to the DM density square map.

Since DM radio emissions would be the result of synchrotron radation emitted by electrons produced in annihilation/decay processes, it is preferable to consider models of secondary electrons from DM annihilation process to determine the origin of relativistic electrons which are belived to be responsible for radio emission in galaxy clusters. The radio emission depends on the shape of the electrons spectrum, that in turn depends on the DM annihilation channel and mass. The annihilation channel in fact determines the nature and the energy of the secondary particles that are produced during the annihilation and that later decay into electrons/positrons,

and this determines the energy that electrons can take, and therefore their energy spectrum. The DM mass determines the maximum energy that electrons can take, and the result is that when the electrons spectrum is approaching that energy, the spectrum steepens quickly and become zero at that energy.

The comparison of our results with the expected value in the previous work [54] is required to confirm our prediction about radio emission from the annihilation of DM into different channels. A 9 or 60 GeV supersymmetric particle is expected to annihilate in quarks and leptons. Direct annihilation into light fermions is helicity-suppressed, so that the main remaining channels of an- nihilations are $b\bar{b}$ and $\tau^{-}\tau^{+}$. Electrons and positrons will con-sequently be mainly produced through secondary processes of hadronization and/or decay. In addition to the a forementioned channels, a 500 GeV supersymmetric particle can also annihilate into gauge bosons, heavy quarks, and Higgs particles. In conclusion, we showed that the shape of the electrons spectrum for a DM particle with mass 9 Gev annihilating into $b\bar{b}$ bestfits the spectral shape of the radio halo of the Coma cluster observed by [54]. The shapes of integrated radio spectrum for intermediate mass neutralinos were nearly consistent for small frequencies. However, the shape of radio spectrum or the flux obtained for higher neutralino masses are lower than the ones obtained in other cases. This is due to, the fact that the electron spectrum is proportional to the square of DM particle mass in general. Hence, possibility of interpreting the origin of radio emission in galaxy clusters with DM annihilation scenario requires a low neutralino mass.

Bibliography

[1] Leite, Natacha and Reuben, Robin and Sigl, Günter and Tytgat, Michel HG and Vollmann, Martin Synchrotron emission from dark matter in galactic subhalos. A look into the Smith cloud Journal of Cosmology and Astroparticle Physics, volume 2016, number 11, year 2016, publisher IOP Publishing

[2] Colafrancesco, Sergio and Regis, Marco and Marchegiani, Paolo and Beck, Geoff and Beck, Rainer and Zechlin, Hannes and Lobanov, Andrei and Horns, Dieter, Probing the nature of Dark Matter with the SKA arXiv preprint arXiv:1502.03738 :2015

[3] Nassim Bozorgnia The Dark Matter Mystery Max-Planck-Institut $f\ddot{u}$rKernphysik, Saupfercheckweg 1, 69117 Heidelberg, Germany

[4] Scott, Pat Searches for Particle Dark Matter: Dark stars, dark galaxies, dark halos and global supersymmetric fits Department of Physics, Stockholm University :2010

[5] Basu, Baidyanath and Chattopadhyay, Tanuka and Biswas, Sudhindra Nath An introduction to Astrophysics publisher : PHI Learning Pvt. Ltd. , 2010

[6] Serway, Raymond A and Moses, Clement J and Moyer, Curt A Modern physics publisher: Cengage Learning ,2004

[7] Roos, Matts Introduction to cosmology John Wiley & Sons ,2015

[8] Basu, Baidyanath and Chattopadhyay, Tanuka and Biswas, Sudhindra Nath An introduction to Astrophysics PHI Learning Pvt. Ltd. ,2010

[9] Nassim Bozorgnia The Dark Matter Mystery Max-Planck-Institut $f\ddot{u}$rKernphysik, Saupfercheckweg 1, 69117 Heidelberg, Germany

[10] Tucci, James V The search for dark matter annihilation in galaxy clusters at VERITAS year 2016

[11] Percival, Will J and Reid, Beth A and Eisenstein, Daniel J and Bahcall, Neta A and Budavari, Tamas and Frieman, Joshua A and Fukugita, Masataka and Gunn, James E and Ivezić, Željko and Knapp, Gillian R and others Baryon acoustic oscillations in the Sloan Digital Sky Survey data release 7 galaxy sample journal : Monthly Notices of the Royal Astronomical Society,volume 401,pages2148–2168 year,2010,

[12] Nassim Bozorgnia The Dark Matter Mystery Max-Planck-Institut $f\ddot{u}$rKernphysik, Saupfercheckweg 1, 69117 Heidelberg, Germany

[13] Gao, L and Frenk, CS and Boylan-Kolchin, M and Jenkins, A and Springel, V and White, SDM The statistics of the subhalo abundance of dark matter haloes Monthly Notices of the Royal Astronomical Society,volume:410 ,The Royal Astronomical Society,2011

[14] Penzias, Arno A and Wilson, Robert Woodrow A measurement of excess antenna temperature at 4080 Mc/s The Astrophysical Journa:volume:142,year :1965

[15] Mather, John C and Cheng, ES and Cottingham, DA and Eplee Jr, RE and Fixsen, DJ and Hewagama, T and Isaacman, RB and Jensen, KA and Meyer, SS and Noerdlinger, PD and others Measurement of the cosmic microwave background spectrum by the COBE FIRAS instrument The Astrophysical Journal:volume,420 ,year :1994

[16] Fixsen, DJ and Cheng, ES and Gales, JM and Mather, John C and Shafer, RA and Wright, EL The cosmic microwave background spectrum from the full cobe* firas data se The Astrophysical Journal, volume 473,year 1996

[17] Colafrancesco, Sergio Dark matter in modern cosmology Aip conference proceedings, volume 1206, number 1, pages 5–26, year 2010, organization AIP

[18] Wilkinson, PN and Henstock, DR and Browne, IWA and Polatidis, AG and Augusto, P and Readhead, ACS and Pearson, TJ and Xu, W and Taylor, GB and Vermeulen, RC Limits on the cosmological abundance of supermassive compact objects from a search for multiple imaging in compact radio sources journal Physical Review Letters, volume 86, number 4, pages 584, year 2001, publisher APS

[19] Alcock, Ch and Akerlof, Carl W and Allsman, RA and Axelrod, TS and Bennett, DP and Chan, S and Cook, KH and Freeman, KC and Griest, K and Marshall, SL and others Possible gravitational microlensing of a star in the Large Magellanic Cloud nature, volume 365, number 6447, pages 621, year 1993, Nature Publishing Group

[20] High energy astrophysics: vol. 1 Longair, Malcolm S Comments on Astrophysics, volume 17, year 1994,

[21] Mueller, Christian M Cosmological bounds on the equation of state of dark matter Physical Review D, volume 71, number 4, pages 047302, year 2005, publisher APS

[22] Klasen, Michael and Pohl, Martin and Sigl, Günter Indirect and direct search for dark matter Progress in Particle and Nuclear Physics, volume:85, pages 1–32 : 2015,publisher:Elsevier

[23] Nozari, Kourosh and Saghafi, Sara and Kamali, Ataollah Damavandi Black hole thermodynamics with a modified dispersion relation admitting minimal length and maximal momentum journal Astrophysics and Space Science, volume 357, number 2, pages 140, year 2015, publisher Springer

[24] Mustafayev, Azar Phenomenology of supergravity models with non-universal scalar masses year 2006, publisher The Florida State University

[25] Feretti, Luigina and Giovannini, Gabriele and Govoni, Federica and Murgia, Matteo Clusters of galaxies: observational properties of the diffuse radio emission journal The Astronomy and Astrophysics Review, volume 20, number 1, pages 54 year 22, publisher Springer

[26] Storm, Emma and Jeltema, Tesla E and Profumo, Stefano and Rudnick, Lawrence Constraints on dark matter annihilation in clusters of galaxies from diffuse radio emission The Astrophysical Journal, volume 768, number 2, pages 106, year 2013, IOP Publishing

[27] Emma Storm. Nonthermal Emission from Galaxy Clusters. PhD thesis, UC Santa Cruz, 2015.

[28] Mekuria, Remudin Reshid and Marchegiani, Paolo and Faltenbacher, Andreas and Colafrancesco, Sergio Multi-wavelength emissions from dark matter

annihilation processes in galaxy clusters using cosmological simulations PoS, pages 009, year 2017, publisher SISSA

[29] Sergio Colafrancesco, Stefano Profumo, and Piero Ullio. Multi-frequency analysis of neutralino dark matter annihilations in the coma cluster. Astronomy & Astrophysics, 455(1):21–43, 2006.

[30] Pasquale Blasi. Cosmic ray acceleration during large scale structure formation. arXiv preprint astro-ph/0412572, 2004.

[31] Luigina Feretti, C Burigana, and TA Enßlin. Diffuse radio emission from the intracluster medium. New Astronomy Reviews, 48(11-12):1137–1144, 2004.

[32] Pasquale Blasi and Sergio Colafrancesco. Cosmic rays, radio halos and nonthermal x-ray emission in clusters of galaxies. Astroparticle Physics, 12(3):169–183, 1999.

[33] L O'C Drury. An introduction to the theory of diffusive shock acceleration of energetic particles in tenuous plasmas. Reports on Progress in Physics, 46(8):973, 1983.

[34] Gianfranco Brunetti, Pasquale Blasi, Rossella Cassano, and Stefano Gabici. Alfvénic reacceleration of relativistic particles in galaxy clusters: Mhd waves, leptons and hadrons. Monthly Notices of the Royal Astronomical Society, 350(4):1174–1194, 2004.

[35] Luigina Feretti. Non-thermal emission from the intracluster medium. Advances in Space Research, 36(4):729–737, 2005.

[36] Gianfranco Brunetti. Modelling the non-thermal emission from galaxy clusters. Arxiv preprint astro-ph/0208074, 2002.

[37] B Dennison. Formation of radio halos in clusters of galaxies from cosmic-ray protons. The Astrophysical Journal, 239:L93–L96, 1980.

[38] Hugo Alberto Ayala Solares. Search for high-energy gamma rays in the northern fermi bubble region with the hawc observatory. 2017.

[39] Anna Kathinka Dalland Evans. Mapping Dark Matter and Dark Energy. PhD thesis, University of Oslo Oslo, Norway, 2009.

[40] Ruphy, Stéphanie Limits to modeling: Balancing ambition and outcome in astrophysics and cosmology ruphy2011limits,volume 42,number 2, year 2011

[41] Springel, Volker The cosmological simulation code GADGET-2 Monthly notices of the royal astronomical society, volume 364, number 4, pages 1105–1134, year 2005, publisher The Royal Astronomical Society

[42] Klypin, Anatoly A and Trujillo-Gomez, Sebastian and Primack, Joel Dark matter halos in the standard cosmological model: Results from the bolshoi simulation The Astrophysical Journal, volume 740, number 2, year 2011, publisher IOP Publishing

[43] Rodríguez-Puebla, Aldo and Behroozi, Peter and Primack, Joel and Klypin, Anatoly and Lee, Christoph and Hellinger, Doug Rodríguez-Puebla, Aldo and Behroozi, Peter and Primack, Joel and Klypin, Anatoly and Lee, Christoph and Hellinger, Doug Monthly Notices of the Royal Astronomical Society, volume 462, number 1, year 2016, The Royal Astronomical Society

[44] Federico Sembolini, Gustavo Yepes, Marco De Petris, Stefan Gottlöber, Luca Lamagna, and Barbara Comis. The music of galaxy clusters–i. baryon properties and scaling relations of the thermal sunyaev–zel'dovich effect. Monthly Notices of the Royal Astronomical Society, 429(1):323–343, 2012.

[45] P Gondolo, J Edsjo, P Ullio, L Bergstrom, M Schelke, and EA Baltz. Darksusy: Computing supersymmetric dark matter properties numerically j. cosmol. Astropart. Phys. JCAP07 (2004), 8, 2004.

[46] Chan, Man Ho and Cui, Lang and Liu, Jun and Leung, Chun Sing Ruling Out 100–300 GeV Thermal Relic Annihilating Dark Matter by Radio Observation of the Andromeda Galaxy
The Astrophysical Journal, volume 872, number 2, year 2019, publisher IOP Publishing

[47] Colafrancesco, S and Marchegiani, P and Beck, G Evolution of dark matter halos and their radio emissions
Journal of Cosmology and Astroparticle Physics, volume 2015, number 02, pages 032, year 2015, publisher IOP Publishing

[48] Bonafede,A and Feretti, L and Murgia, M and Govoni, F and Giovannini, G and Dallacasa, D and Dolag, K and Taylor, GB The Coma cluster magnetic field from Faraday rotation measures Astronomy & Astrophysics, volume 513, pages A30, year 2010, publisher EDP Sciences

[49] High energy astrophysics: vol. 1 Longair, Malcolm S Comments on Astrophysics, volume 17, year 1994,

[50] Volker Springel. Smoothed particle hydrodynamics in astrophysics. Annual Review of Astronomy and Astrophysics, 48:391–430, 2010.

[51] Proper, Megan Longo Dark Matter annihilation cross-section limits of dwarf spheroidal galaxies with the High Altitude Water Cherenkov (HAWC) gamma-ray observatory and on the design of a water Cherenkov detector prototype year 2016, Colorado State University. Libraries

[52] Aartsen, MG and Ackermann, M and Adams, J and Aguilar, JA and Ahlers, M and Ahrens, M and Altmann, D and Anderson, T and Arguelles, C and Arlen, TC and others Observation of high-energy astrophysical neutrinos in three years of IceCube data Physical review letters,volume 113 ,number 10 ,year 2014 ,publisher APS

[53] Sembolini, Federico and Yepes, Gustavo and De Petris, Marco and Gottlöber, Stefan and Lamagna, Luca and Comis, Barbara Erratum: The MUSIC of galaxy clusters-I. Baryon properties and scaling relations of the thermal Sunyaev-Zel'dovich effect Monthly Notices of the Royal Astronomical Society, volume 434, pages 2718–2719, year 2013

[54] Thierbach, M and Klein, U and Wielebinski, R The diffuse radio emission from the Coma cluster at 2.675 GHz and 4.85 GHz Astronomy & Astrophysics, volume 397, number 1, pages 53–61, year 2003, publisher EDP Sciences

DECLARATION

ADDIS ABABA UNIVERSITY
COLLEGE OF NATURAL AND COMPUTATIONAL SCIENCES
DEPARTMENT OF PHYSICS

MSc Thesis

Exploring different neutralino dark matter annihilation channels in radio frequency emission in simulated coma like galaxy cluster

Name of Candidate: Jemal Regasa Mashura

I the under signed declare that the thesis is my original work and no part of it can be claimed as an intellectual property of anybody else except me and my advisors.

Signature: _____